(2) The spreading center extended from the Willaumez rise to the eastern part of the New Guinea Basin is a ridge trending S35°W, having a length of about 76 km, a width of about 5~15 km and depth of about 750~1,750 m. Its axial valley is intermittent and is within the bounds of possibility that the central valley is distributed in echelon or in a row (see Figure 5-2-3).

(3) As shown in Figure 3-3-1, it is possible to interpret the ridge on the western part as a dying spreading center, as a continuation of the spreading center described in paragraph (1), and the ridge on the eastern side as a propagating spreading center, but we don't adopt these as spreading centers for the following reasons.

That is, if we introduce (3), then there would be two series of spreading centers roughly in parallel, which could be considered as the so-called overlapping spreading center(*1). Therefore, if we arrange a transform fault zone trending N80°W between these two series, it would be contradictory to the plate tectonics theory. This point is a theme to be solved in the future.

(4) We presumed two transform fault zones within the Willaumez rise. They trend northwest, which is the almost same direction as that of the rise crest. Their trends are N72°W and N80°W, respectively.

(5) In the New Guinea Basin, the transform fault zones shift their course from N60°W toward east and west in the neighborhood of 3°20'S, 146°30'E. A belt-shaped shallow earthquake zone trending E-W is distributed in this area. The topography of the transform fault zone trending N60°W assumes, in the main, cliff-typed furrows and the topography of the transform fault zone trending E-W assumes small seamounts and seamount chains.

(*1) In comparison with the overlapping spreading center discovered on the East Pacific Rise, the two circular furrows lying between the two spreading centers are too wide to be regarded as overlap basins (deep holes). For the reason that it corresponds to conspicuous magnetic anomalies, we concluded that it must be a transform fault zone.

According to Eguchi (1989) and Taylor et al. (1991), the earthquake focal mechanism solution of the shallow earthquake in the Bismarck Sea is a strike-slip type solution and the transform fault zone is accompanied by a spreading center. It, therefore, is a theme to be solved whether the transform fault zones (3) and (4) are also accompanied by spreading centers.

We cannot specify the starting age nor the opening rate (spreading rate) of the spreading as we cannot identify the magnetic Stripes.

The relation between the spreading system and the magnetic anomalies is as follows;

The spreading center (1) belongs to a low magnetization zone extending from north to south. The spreading center (2) belongs to a low magnetization zone (below 5 A/m) trending, as a whole, north and south.

However, conspicuous magnetic anomalies (such as magnetic stripes) reflecting the two spreading centers are not recognized.

The propagating spreading center and the dying spreading center belong to medium magnetization zones with roughly the same values of about 5 ~ 10 A/m and no difference is recognized between the propagating spreading center and the dying spreading center. Furthermore, no magnetic structure that reflects both spreading centers is recognized.

As for the reasons that the spreading centers in this area belong to low magnetization zones while the neovolcanic zones found on the summits of the East Pacific Ridge belong to high magnetization zones, we can point out that the sea-floor spreading and the volcanic activity ceased for a long time, thus no lava was freshly supplied. The spreading center (1), however, can also be interpreted as demagnetization caused by the hydrothermal alteration.

The two transform fault zones in the Willaumez rise correspond to a conspicuous linear and low magnetization zone. On the northern side of the transform fault zone that runs the New Guinea Basin in the northwest direction has a tendency to be attended by high magnetization zones at a part of it. On the magnetic anomaly map, the transform fault zone that runs from east to west is located in the neighborhood of the boundary between the positive and negative magnetic anomalies (its amplitude is small) and, contrasting with the transform fault zone in the Willaumez rise, it does not show conspicuous magnetic anomalies. We can infer the reason to be that the transform fault zones in the New Guinea Basin have few volcanic activities. Furthermore, this area roughly coincides with a district in which belt-shaped shallow earthquake trending east

and west was observed, which suggests that the plate is a rigid body.

<Willaumez rise>

As described in paragraph 3-1, the Willaumez rise has a width of 60~70 km, extends in the northwestern direction and is shallower than about 1,500 m in water depth.

The east boundary of the Willaumez rise forms a steep cliff with a relative height difference of about 1,000 m and a high magnetization zone exists along the boundary. Above-mentioned spreading centers (ridges) and a dying spreading center (ridge) exist roughly in the southwest of the west boundary but no obvious steep cliffs are recognized. On the magnetic structure map (Figure 3-2-7), however, the depth of occurrence of magnetic substances is elevated than in the Manus and New Guinea Basins, the west boundary also assumes a steep cliff trending roughly in the north and south direction and the Willaumez rise shows a horst structure extending in the northwest direction.

Also, there exist a transform fault trending the same direction with the rise crest, a spreading center crossing the rise crest orthogonally, and a propagating spreading center, and this rise is considered to be a rise with a complicated tectogenesis.

There are a plenty of reefs and seamounts/ridges with summits at the depth of about 600 m within the rise. Also, high magnetized substances are distributed in the rise, from which we can infer the existence of concealed dikes as well as the local existence of large and small non-magnetic substances produced by the hydrothermal process. From this we can consider that the Willaumez rise used to be a rise with violent volcanic activities. We can infer that a part of these volcanic activities is closely related with the transform faults.

We could not identify the age of the seafloor as we could not idenfy the magnetic stripes. However, from the facts that magnetic substances are widely distributed in the seafloor, that, according to the FDC observation, the sediments are thin and that ore signs are discovered from the area, we can consider that there are many relatively new volcanoes in this area.

Johnson (1979) considers that the Willaumez rise was elevated by the diapirism (the density of the mantle at a high temperature is smaller than that of crusts) caused by the tectonic uplift before 3.5 Ma by enumerating the (1) extinct spreading center, (2) remnant arc and (3) hot spot trace.

<New Guinea Basin>

(1) The existence of a magnetic structure with low magnetization trending NW is presumed between 147°00'E~147°20'E.

(2) The south side of the transform fault zone is a very flat seafloor with few seamounts. However, the magnetic structure corresponding to the magnetization zones (Figure 3-2-6) of about 10 A/m - which is distributed in belt-shape and scattered-points-shape on the south side - is presumed to be buried in the sediments. Also, the seamount located in the neighborhood of 3°35'S, 146°43'E shows normally magnetized magnetic anomalies.

(3) A water depth of 2,400 m, the deepest place in the survey area, is located in the neighborhood of 3°20'S, 146°40'E. Positively magnetized magnetic anomalies with high magnetization, extending from south to north, is recognized in and around the deepest place (Figure 3-2-5). From which the existence of fresh lava is inferred.

(4) The seamount located in the vicinity of 3°18'S, 145°48'E on the north side of the transform fault zone is within the negative magnetic anomalies.

Chapter 4. Geochemical Survey

4-1 Outline

This year's geochemical survey consists of "Regional geochemical sampling" and "Base-line geochemical sampling".

For the Regional geochemical sampling, an aggregate of 39 sampling points was established. These sampling points were established at 30' grid within the waters encircled by longitude and latitude of 2°30'S, 4°00'S, 145°30'E and 148°00'E, by adding one sampling point at the center of each grid.

As for the Base-line geochemical sampling, line-shaped sampling points were established in the orthogonal direction to the direction of the FDC track lines centering around the ore signs or indications of the 92SFDC02 track line (3°24.70'S, 147°03.81'E) and the 92SFDC06 track line (2°57.32'S, 147°26.55'E). These ore signs or indications had been discovered in the course of the FDC survey carried out at the axial part of the ridges (whose existence was estimated by theresults of the topographical survey). The former line is named as "Base-line A" and the latter "Base-line B." The former is located on the south-western side and the latter on the northeastern side. As the Base-line B intersects with the dying spreading center at "3°10.57'S, 147°37.63'E," this point was adopted as the secondcenter of this line. The former ore signsor indications were named as the first center, thus double center was established on this line (Base-line B). As a result, sampling points of the Base-line A were established from the above-mentioned ore signs or indications in the directions of 126° and 306°. These samplingpoints are located at distances of 1.0 mile, 2.5 miles, 5.0 miles, 7.5 miles, 10.0 miles, 15.0 miles and 20.0 miles from the center. However, the center point was excluded from the planned points as samples had already been collected from this point when the sampling for hydrothermal ore deposits was carried out. Sampling points for the Base-line B were established in the line directions of 141° (321°) at distances of 1.0 mile, 2.5 miles, 5.0 miles, 7.5 miles and 10.0 miles northeastward and 1.0 mile and 2.5 miles southeastward from the first center, as well as 1.0 mile, 2.5 miles and 5.0 miles northeastward and 1.0 mile, 2.5 miles, 5.0 miles, 7.5 miles and 10.0 miles southeastward from the second center. Planned sampling points for the Base-lines A and B amounted to 14 points and 16 points respect-ively. The total of them are 30 points.

As for the samplers, a gravity corer (a large corer was used in the early stage) was mainly used. Sampling efforts were continuously made by employing an ocean grab or a power grab at the points where samples were not collectable by the gravity corer.

However, the sampling efforts were abandoned when no samples were collectable even by these two trials.

In consequence, the regional geochemical sampling succeeded at every planned point, while the base-line geochemical sampling failed at 3 points. These 3 points include one point on the Base-line A (the point 1.0 mile northwestward from the center) and two points on the Base-line B (2.5 miles north-westward from the first center and the second center.)

The regional geochemical sampling points are indicated by the latter two figures of the fiscal year (92) + R (means "regional") + equipment used (two alphabetical letters) + serial numbers in two figures. Employed equipment is indicated by GC (gravity corer), LC (large corer), OG (okeangrab) or PG (finder mounted power grab). Accordingly, the firstsampling point employing the large corer is represented by "92RLC01".

The base-line geochemical sampling points are indicated by the latter two figures of the fiscal year (92) + B (means "base-line") + equipment used (two alphabetical letters) + serial numbers in two figures. Employed equipment is indicated, in the same way as in the case of the regional geochemical sampling, by GC (gravity corer), OG (okean grab) and PG (finder mounted power grab). As the sampling operation of the base-line B was carried out first, the sampling points of the base-line B were numbered from 01 to 16 and sampling points of the base-line A were numbered from 17 to 30. Accordingly, the first sampling point of the base line A employing the gravity corer is represented by "92BGC17." Furthermore, the three unsuccessful sampling points are treated as missing numbers, so the serial numbers of 06, 10 and 23 are non-existent numbers.

Locations of the sampling points are described, for the sake of convenience, as "R + serial numbers" for the regional geochemical sampling and "B + serial numbers" for the base-line geochemical sampling in the following paragraphs of this Chapter.

Locations of the regional geochemical sampling and the base-line geochemical sampling are shown in figures 4-1-1 and 4-1-2 respectively. The results of the regional geochemical sampling are shown in the Appendix 1. The results of the base-line geochemical sampling are shown in the Appendix 2.

4-2 Characteristics of Samples Collected

Samples collected by the gravity corer and large corer are the columnar cores. Samples collected by the power grab are the columnar cores as columnar samplers are fitted in the grab. Samples collected by the okean grab generally do not take the

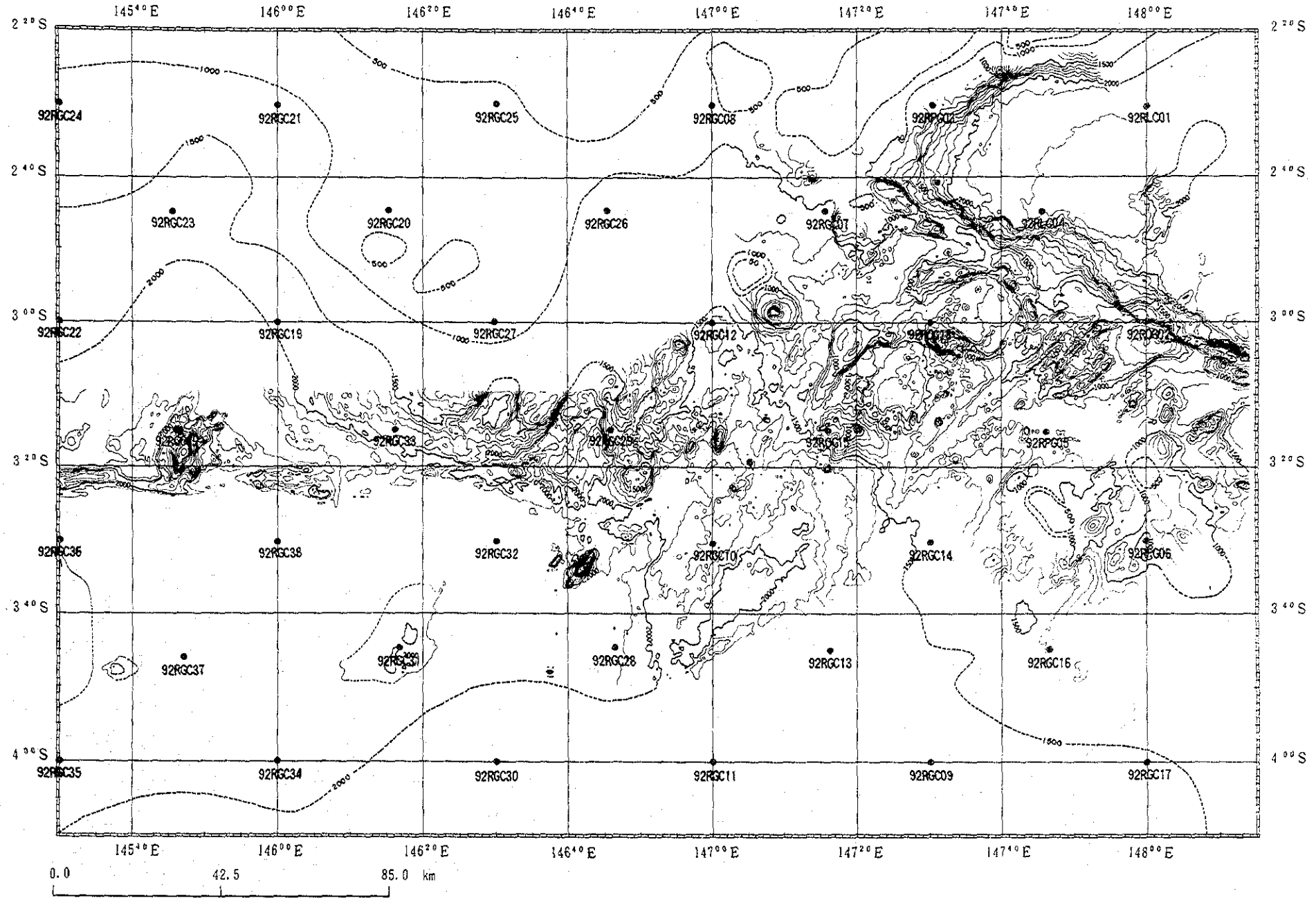

Figure 4-1-1 Location Map of Regional Geochemical Sampling Points

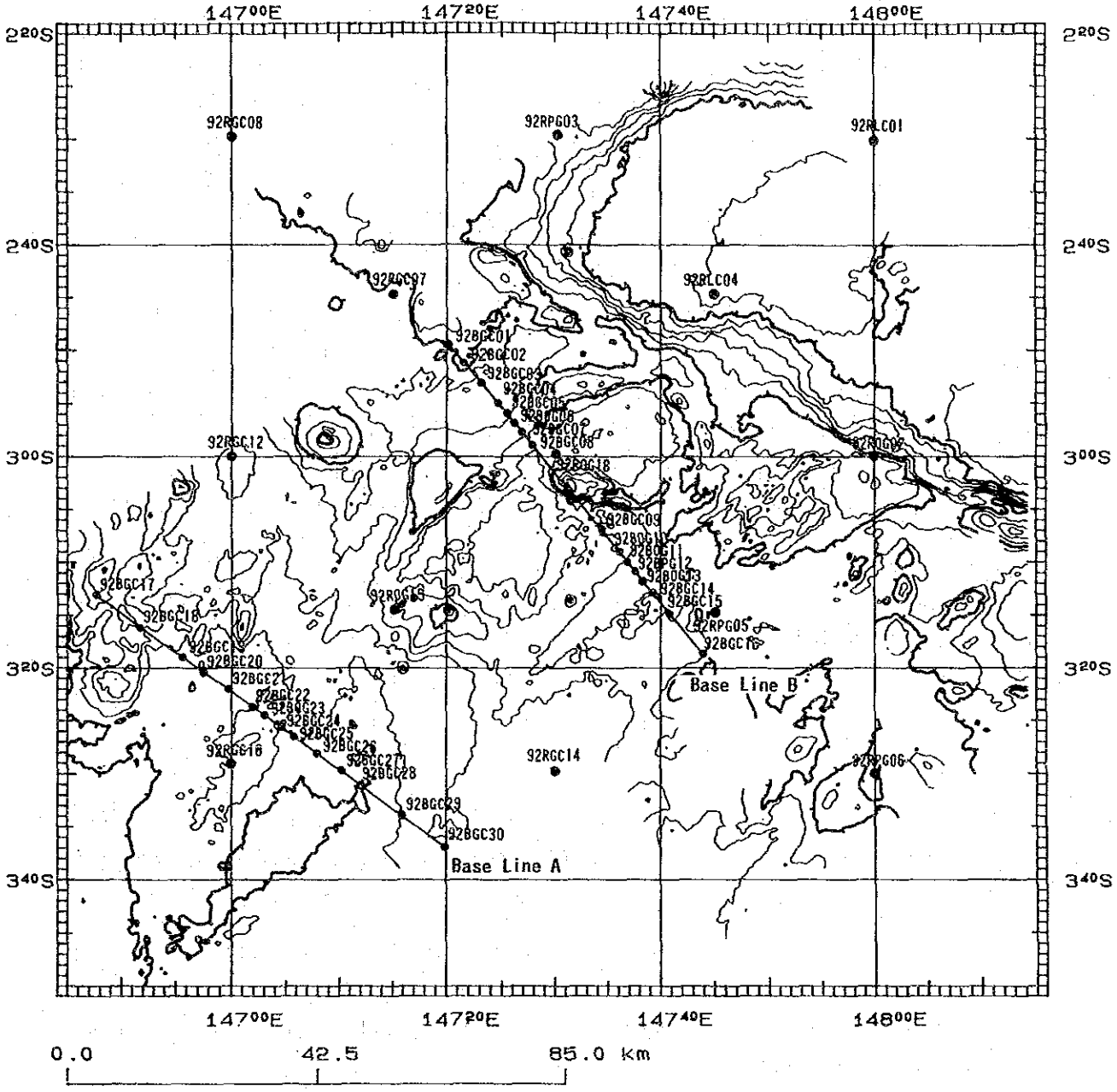

Figure 4-1-2 Location Map of Base Line Geochemical Sampling Points

columnar shape. They were in turbulence form when heaved, but they were changed into columnar shape for sampling when they could be restored to their original state.

In the case of regional geochemical sampling, basalt was collected from, or the bit of the gravity corer was deformed by base rock at eight points out of the total 39 points. Those eight points were located around the presumptive axial zone of the ridges. Only muddy substances were collected from the remaining pointsand no deformation of the gravity corer occurred. Consequently, it is presumed that the thickness of sediments could be more than 2 m, which is the collectable depth of the corer.

On the other hand, basalt was collected from, or the bit of the gravity corer was deformed by base rock at 10 points out of the 14 points on the Base-line A (including uncollect-ablecases) and 14 points out of the 16 points on the Base-line B (including uncollectable cases) in the case of base-line geochemical sampling, which was carried out in the form of traversing the presumptive axial zone of the ridges. The length of sampled muddy substances has a tendency to get extremely short atpoints near the centers of the two track lines.

Sampled columnar cores were sketched in columnar view first and then divided into two portions. One of them was appropriated to chemical analysis, X-ray diffraction and other analyses, and the remaining portion was preserved.

1) Muddy Substances

Sampled muddy substances were mainly classified by their color tones and grain size. "MUNSELL SOIL COLOR CHARTS" were employed to classify the color tone. A Wentworth (1922) grain size scale was employed to classify the grain size.

Color tones of the sampled muddy substances are mainly composed of the 10YR series (brownish series) and 5Y series (olive series) of the "MUNSELL SOIL COLOR CHARTS". Grain size is mainly composed of clay ~ medium sand of the Wentworth (1922) grain size scale.

The main composition of muddy substances are volcanic glass, calcareous foraminifera shells and clay. Their quantitative ratio constitutes the decision factors of the above mentioned classification. In addition to these main composition, clastic fragments of such minerals as quartz, plagioclase, pyroxene, amphibole, etc., and such microfossils as radiolaria and sponge spicules are contained in muddy substances as subcomposition. No authigenic minerals are recognized.

Volcanic glass recognized in muddy substances of these waters can be roughy classified into two types. They are mafic glass and felsic glass. Mafic glass is overwhelmingly abundant in quantity while the existence of felsic glass is rarely identified. However, when mafic glass exists in muddy substances, their mafic glass content does not exceed 50% except for special cases, but when felsic glass exists in muddy substances, felsic glass tends to form a stratum of its own. The felsic glass content in such a stratum will be almost pure. As such a stratum hardly holds other composition, so it can be a key bed when making a stratigraphical analysis.

Mafic glass assumes black (in the case of thicker layers) ~ brown (thinner ones) colors. Sizes of mafic glass samples vary from several μm ~ macroscopic size but are relatively well sorted in the sample scale. It seems that a large number of samples have approximately 20 μm-sized glass when examined with a microscope. Morphologically, small plate type fragments with frothy inner structure are most numerous, but some of the samples have the structure of pipe-shaped holes bundled in parallel or porous fragmentary structure.

Felsic glass assumes a transparent ~ white translucent color. Sizes of felsic glass samples are smaller than 100 μm and mean diameters of such samples are slightly larger than those of the mafic glass. A morphological characteristic of felsic glass samples is the structure with a lot of spherical froth and pipe-shaped froth.

Calcareous foraminifera shells assume a white color. Sizes of them are between 50 μm and 1 mm, but larger shells are observed only as fragments when examined with a microscope. The content of calcareous foraminifera shells in muddy substances does not exceed 20%. As most of the patterns of chamber arrangement of planktonic foraminifera are trochoidal circling ~ flat circling ~ double-line-shaped, it is presumed that a lot of them belong to the plaktonic foraminifera's Upper Globigerinacea Family. Identification of foraminiferal fossils was performed regarding 3 samples of sediments taken from this sea area, in order to estimate the age of sedimentation, the velocity of accumulation and the paleo-environment of sedimentation. The result of identification of foraminiferal fossils revealed that the sedimentation age of 3 samples were late Pliocene, Diluvium (later than 690 million years BP) and the second half of early Pliocene, and the velocity of accumulation was also estimated 0.4 ~ 1.6 mm/1000 years based on the assumption of no hiatus. The details of identification method would be described later in this section.

Much of the sampled clay has a brown color tone. Due to its small size in grains, it is difficult to examine it with a microscope. However, from the fact that muddy substances composed of nothing but clay were not collected from this year's sampling and most of them were accompanied, to a certain degree, with volcanic glass and clastic minerals, the source of the clay is supposed to be volcanic glass and clastic minerals. In most cases, flocculation in clay is formed around foraminifera's calcareous shells and volcanic glass as its cores.

Among clastic minerals, quartz and plagioclase are universally contained, though a small amount, in almost all muddy substances. Pyroxene and amphibole are also universally recognized when the amount of quartz and plagioclase increases. All of them are considerably fresh. When the amount of volcanic glass in normal muddy substances increases, the size of volcanic glass becomes larger, and in proportion to that, the amount and size of these clastic minerals go on increasing. And, finally, they will change to volcanic ashes containing only volcanic glass and clastic minerals. Therefore, it may well be that these clastic minerals are volcanic minerals. The size of these clastic minerals varies from several μm to 500 μm but, in normal muddy substances, their diameters are, in general, less than 50 μm.

A small amount of siliceous microfossils like radiolaria and sponge spicules are observed ubiquitously. The size of radiolaria is about 100 μm and many of them are Euchitonia, which indicates the tropical community. In most cases, the length of sponge spicules are several tens to hundreds μm when observed with a microscope, but there are some with macroscopic length of several cm.

In addition to the above, occurrence of shells of snails and bivalves are recognized especially at places where calcareous shells of foraminifera are abundant.

Vertical distribution patterns of muddy substances at the greatest common divisor recognized in these waters can be classified into three layers. The surface layer is olive grey ~ grey sediments suffused with water, the middle layer is dark brown ~ brown sediments and the bottom layer is olive grey ~ grey sediments partially containing black ~ dark grey volcanic ashes.

The olive grey ~ grey sediments suffused with water, i.e. the surface layer, are composed of relatively abundant calcareous foraminifera shells and clay/volcanic glass. These sediments are uncoagulated mud, and flocculation of clay is not recognized. They assume a grey color when the volume of volcanic glass increases relatively. Many sampling points are short of this layer.

The dark brown ~ brown sediments (middle layer) contain considerable amounts of clay and fine grain mafic glass but very few of calcareous foraminifera shells.

Among the olive grey ~ grey sediments partially containing black ~ dark grey volcanic ashes, the olive grey ~ grey portion is composed of relatively abundant calcareous foraminifera shells and clay/volcanic glass. Flocculation of clay with calcareous foraminifera shells as core is recognized. Grains of partially contained black ~ dark grey volcanic ashes are relatively coarse and most of them are medium-grained sand ~ silt-sized. The composition of these volcanic ashes are volcanic glass and clastic minerals. Most of them do not contain calcareous foraminifera shells and, in general, no clay is contained. Such normal grading as changing from black~ dark grey volcanic ash layer up to olive grey ~ grey sediments is recognized occasionally.

Horizontal distribution patterns of the muddy substances in these waters are discussed hereunder on the basis of the columnar chart of the samples collected through the regional geochemical sampling. (Fig. 4-2-1-1). It was not easy to correlate cross-sections between neighboring points even in the case of the base-line geochemical sampling - in which samples were collected at intervals of several miles. Therefore, it is impossible to strictly correlate the stratums in the regional geochemical sampling - in which sampling was carried out at intervals of around 21 miles. However, different characteristics of muddy substances among areas as described hereunder are conceivable.

Southwestern part: Calcareous foraminifera shells are hardly contained in the samples (R28, R31, R32, R34, R35, R36, R37 and R38) collected from the basin encircled by the isobathymetric line of 2,000 m deep. Black~dark grey volcanic ashes, (silt ~ medium-grained sand-sized) comprised of clastic minerals and volcanic glass, and highly sticky grey clay are predominant. Sediments with such characteristics are different from the above-mentioned ordinary sedimentary pattern.

Southeastern part: Many samples have a white felsic glass layer of several cm thick on the relatively upper part of the third layer of the above-mentioned ordinary sedimentary pattern (R14, R16, R17, B15, B27, B28, B29 and B30). This layer has the possibility to be a key layer but the active source of it is unknown at present.

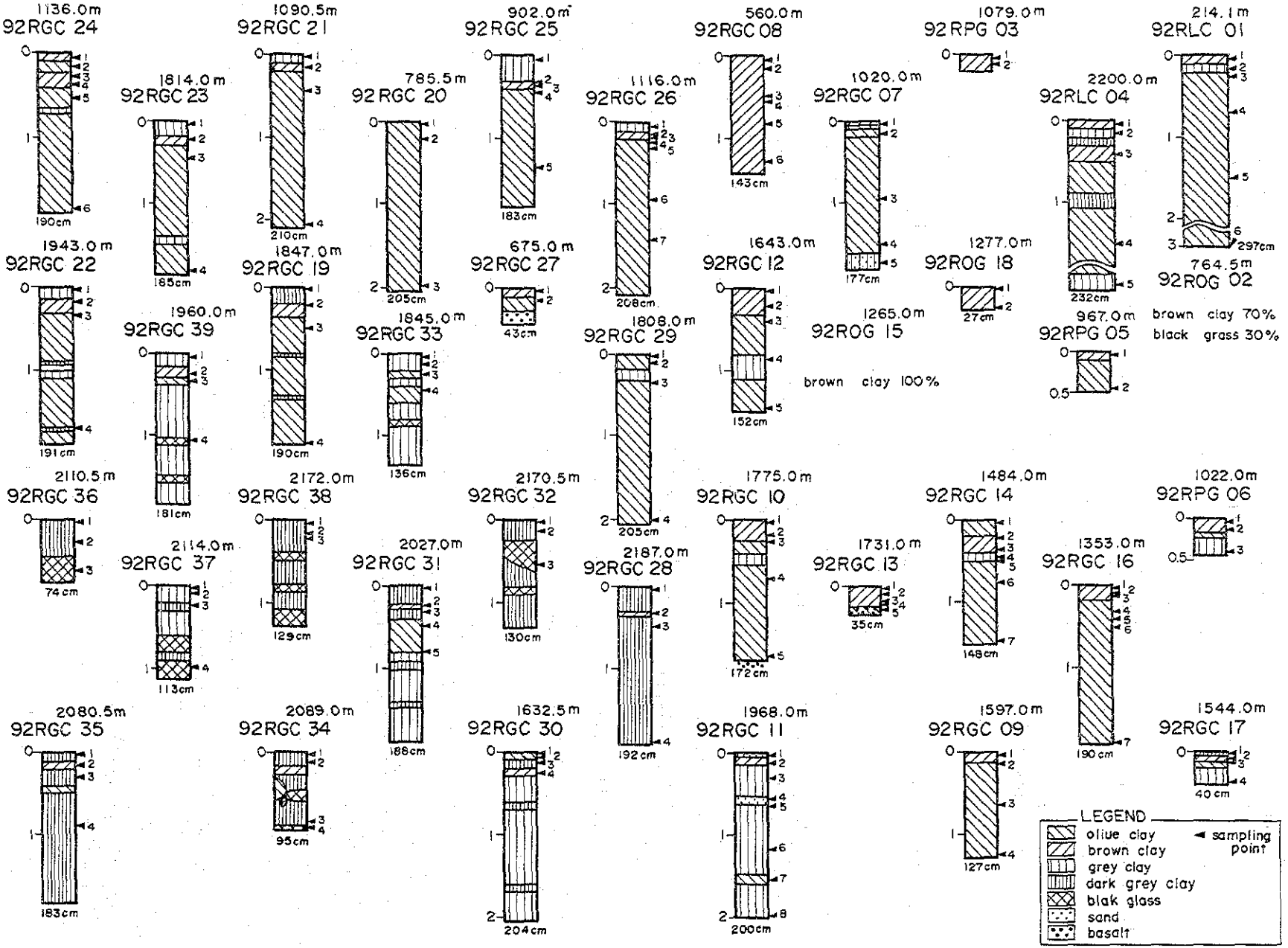

Figure 4-2-1-1 Schematic Drawings of Sampling Results Obtained from Regional Geochemical Survey

<Observation of microfossils on the seabed>

① Specimens for analysis:

The following specimens were analysed.

No.	Sample No.	Depth(cm)	Remarks
301	92RLC01-07	210～220	green (M. No.5Y6/2>5/2) tfs. clay
307	92RGC24-07	110～130	grey(M. No.5Y5/2) clay with much shell fragments
312	92RGC29-05	150～160	olive grey(M. No.5Y5/2) clay

All the specimens are clay, full of planktonic foraminiferal fossils, and no other fossils are seen.

② Analytical method:

Since all the specimens are extremely rich in planktonic foraminiferal fossils, we added warm water to the wet specimen, about 20 grams (as for red clay, we normally use 30 grams since few foraminiferal fossils are contained) and left it for one day to make it muddy; then it was washed through a screen of 150 mesh(=0.125mm) and dried. Under a microscope, it was then scattered over a test plate with grid so that residual particles do not overlap each other. All the individual fossils of planktonic and benthic foraminifera were taken out and identified.

③ Results of identification:

The results of the observation are as follows. A picture of a representative species of foraminiferal fossils is shown in the Figure 4-2-1-2 (1), (2), and the Table 4-2-1-1 is the list of foraminifera thus identified.

[210-220 cm of 92RLC01-07]

Planktonic foraminiferal fossils are rich in number of both species and bodies collected. The condition of preservation is good, too. Only 11 bodies of benthic foraminiferal fossils were recovered.

From this specimen, we can see *Globorotalia tosaensis* which extincts just after the border between Matsuyama Reversed Epoch and Brunhes Normal Epoch. Also, *Neogloboquadrina dutertrei*, which appears after N20 of Blow

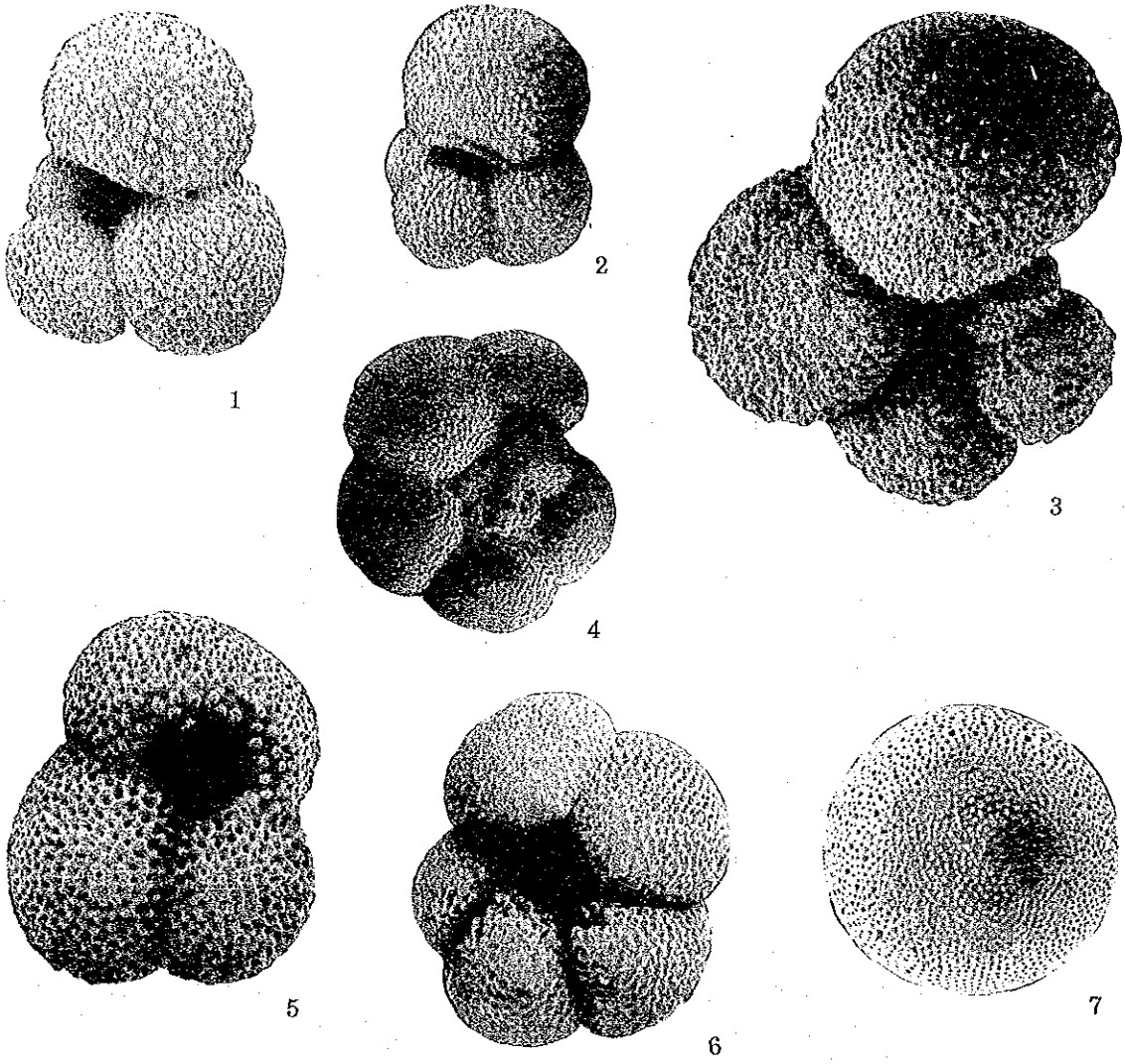

1. *Globigerina bulloides* (92RGC24-07)
2. *Globigerina falconensis* (92RGC29-05)
3. *Globigerinella aequilateralis* (92RLC01-07)
4. *Globigerinoides ruber* (92RGC29-05)
5. *Neogloboquadrina dutertrei* (spiral side, 92RLC01-07)
6. *Neogloboquadrina dutertrei* (ventral side, 92RGC24-07)
7. *Orbulina universa* (92RLC01-07)

(Scale a:5, 7 b:6 c:1~4)

Figure 4-2-1-2 Species of the Typical Foraminiferal Fossils (1)
(Planktonic Foraminifera)

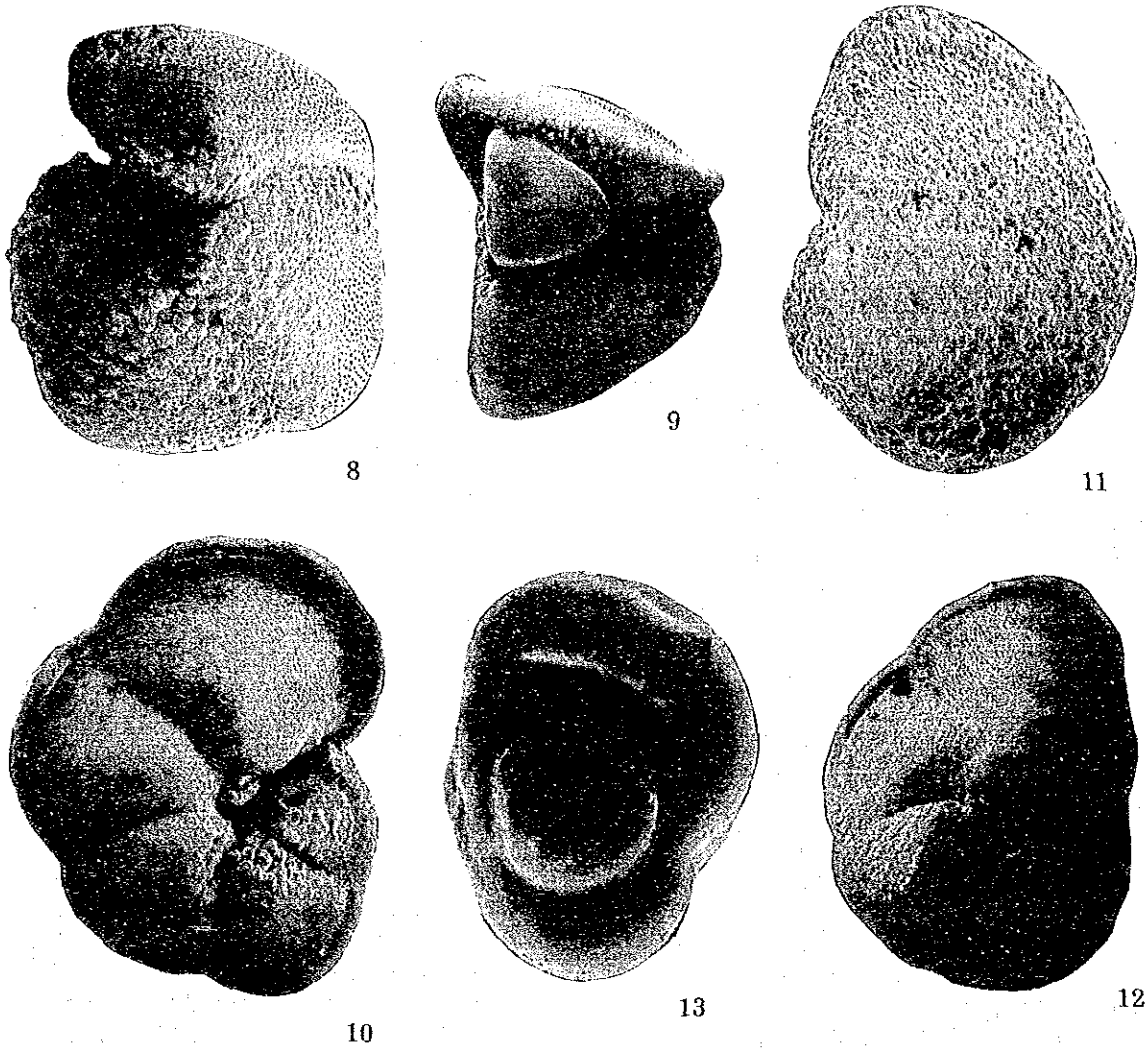

8. *Globorotalia truncatulinoides* (ventral side, 92RGC24-07)
9. *Globorotalia truncatulinoides* (apertural side, 92RGC24-07)
10. *Globorotalia menardii* (92RLC01-07)
11. *Globorotalia tumida* (spiral side, 92RGC29-05)
12. *Globorotalia tumida* (ventral side, 92RGC29-05)
13. *Pulleniatina obliquiloculata* (92RGC29-05)

(Scale a:9, 10, 12 c:11, 13)

Figure 4-2-1-2 Species of the Typical Foraminiferal Fossils (2)
(Planktonic Foraminifera)

Table 4-2-1-1 List of Foraminiferal Fossils

Species \ Samples Depth(m)	92RLC01-07 210-220cm	92RGC24-07 110-130cm	92RGC29-05 150-160cm
(Planktonic Foraminifera)			
Globigerina apertula		7	2
Globigerina bulloides	12	30	35
Globigerina falconensis		8	25
Globigerina foliata	5	4	5
Globigerina spp.		6	1
Globigerinoides conglobatus		2	
Globigerinoides elongatus		2	1
Globigerinoides obliqus		1	
Globigerinoides ruber	18	22	36
Globigerinoides quadrilobatus	12	3	2
Globigerinoides sacculifer	4	4	2
Globigerinoides spp.	3	1	1
Orbulina universa	5	3	1
Globorotalia crassaformis			1
Globorotalia menardii	14	4	9
Globorotalia scitula	1	1	
Globorotalia tosaensis	7		
Globorotalia truncatulinoides		4	
Globorotalia tumida	16	4	18
Globorotalia tumida flexuosa			1
Globorotalia ungulata	1	4	
Globorotalia spp.		3	4
Globoquadrina pseudofoliata	2		
Globoquadrina spp.	1		
Neogloboquadrina dutertrei	24	23	23
Neogloboquadrina cf. dutertrei	19	40	16
Neogloboquadrina spp.	1	2	
Pulleniatina obliquiloculata	54	16	15
Pulleniatina spp.	2		
Globigerinita glutinata	2		2
Globigerinita uvula		2	3
Globigerinita spp.	1		
Globigerinella obesa			6
Globigerinella cf. obesa			1
Globigerinella aequilateralis	12	16	6
Globigerinella spp.			4
(Benthonic Foraminifera)			
Bulimina aculeata	1	1	1
Bulimina striata	1		
Bulimina spp.		1	
Cassidulina carinata		1	
Celatobulimina pacifica		1	
Chilostomella ovoidea		2	
Cibicidoides spp.	2		
Gaudryina bradyi		2	
Gyroidina neosoldanii	1		
Gyroidina spp.	1		1
Haplophragmoides spp.		1	
Hoeglundina elegans	1	2	
Melonis parkerae			1
Planulina wuellerstorfi		1	
Pyrgo serrata		1	
Pyrgo vespertilio	1		
Quinqueloculina spp.	1	1	
Robertinoides bradyi		2	
Triloculina spp.	1		
Uvigerina hispida	1	1	1
Uvigerina spp.		1	
Total Planktonic Foraminifera	216	205	218
Total Benthonic Foraminifera	11	18	4
Total(Planktonic + Benthonic)	227	223	222

frequently. *Globorotalia truncatulinoides* which appear in Quaternary is not seen in these specimens.

As for benthic foraminiferal fossils, *Bulimina aculeata, Bulimina striata, Cibicidoides spp., Gyroidina neosoldanii, Hoeglundina elegans, Pyrgo vespertilio, Uvigerinahispida,* etc have been collected.

In this specimen, we have observed *Globorotalia tosaensis* which sppear in late Pliocene and disappear in early Diluvium (about 690,000 years ago, just after the border line between Matsuyama Reversed Epoch and Brunhes Normal Epoch. Since no *Globorotalia truncatulinoides* which starts to appear only in Quaternary was not seen, the sediments cannot be thought to be Quaternary at least. Moreover, we can observe *Globorotalia ungulata* which starts to appear only in late Pliocene. Therefore, we can assume that the specimen is the sediments of late Pliocene (about 3.1-1.8 million years ago). Since *Globigerina foliata* which became extinct in late Miocene is collected though the amount is very small, the sediments of late Miocene could have been exposed to the neighboring area in late Pliocene.

As to benthic foraminiferal fossils, the number of bodies collected was small and most of them were calcareous foraminifera. Species, such as *Bulimina aculeata, Chilostomella ovoidea, Gyroidina neosoldanii, Hoeglundian elegans, Pyrgo vespertilio, Uvigerina hispida* etc, are all the kind that has a lime shell, and their paleo-water-depth is estimated to have been 1,000-2,000m, which is not much different from the present.

[110-130 cm of 92RGC24-07]

Like 210-220 cm of 92RLC01-07, this specimen is rich in planktonic foraminiferal fossils. *Globorotalia truncatulinoides,* which starts to appear only in Quaternary (about 1.8 million years ago), has been collected, but no *Groborotalia tosaensis* is seen which starts to appear in late Pliocene and became extinct in early Diluvium (about 690,000 year ago, or just after the border between Matsuyama Reversed Epoch and Brunhes Normal Epoch. Therefore, this specimen is thought to be a sediment newer than about 690,000 years ago. The presence of a few planktonic foraminiferal fossils from late Miocene suggests the possibility that the sediments from late Miocene were distributed and exposed on the adjoining sea-bed.

Although only 18 bodies of benthic foraminiferal fossils were found, *Bulimina aculeata, Celatobulimina pacifica, Chilostomella ovoidea, Hoeglundina*

elegans, *Robertinoides bradyi* etc are seen. They are semi-deepsea and deepsea species which reside deeper than several hundred meters, and therefore, we can assume that the paleo-water-depth was at least several hundred meters or deeper.

[150-160 cm of 92RGC29-05]

Planktonic foraminiferal fossils are abundant both in the number of species and in the number of bodies collected. The preservation condition was good, too. The number of bodies of benthic foraminifera is very small, i.e. only four.

This specimen shows *Globigerina apertula* which appears in late Miocene (N16) and disappear in early Pliocene (N20) and *Globorotalia tumida flexuosa* which appears in early Pliocene (N19) and disappear in late Pliocene (N21), but does not show *Groborotalia tosaensis* which appears in late Pliocene (N21) and becomes extinct in early Diluvium (just after the border between Matsuyama Reversed Epoch and Brunhes Normal Epoch. And relatively many a *Pulleniatina obliquiloculata*, which appears in the second half of early Pliocene (N19-20), is seen. All these suggest the strong possibility that the age of the specimen is from the second half of early Pliocene (N19-20).

As for benthic foraminiferal fossils, *Bulimina aculeata*, *Gyroidina spp.*, *Melonis parkerae*, and *Uvigerina hispida* are seen. From the ecological characteristics of these species, we can assume an paleo-water-depth of several hundred to 2,000m deep.

④ Presumption of accumulation speed and old environment:

Since the specimens do not have any foraminiferal data below and above them, we cannot calculate the average accumulation speed accurately. Assuming that there is no hiatus (accumulation gap) between each specimen and the seafloor, the specimen [92RLC-07] gives 0.7-1.1 mm/1000 years, [92RGC24-07] about 1.6 mm/1000 years, and [92RGC29-05] 0.4 mm/1000 years. In general, however, it is difficult to believe that there exists no hiatus (accumulation gap) between the depth of the specimen and the seafloor, and the value which the specimen [92RGC29-05] gives, in particular, is too small to ignore existence of hiatus (accumulation gap).

Every specimen contains a small amount of planktonic foraminiferal fossils of an age older than the estimated accumulation age which the specimen

suggests. We can, therefore, assume that, at the time of accumulation, sediments of an older age were distributed and exposed in the adjacent areas which were relatively higher floor-bed (or land surface).

2) Rocks

As the sampling objects of the regional and base-line geochemical sampling are muddy substances, only a few rocks are included in the samples collected.

In the case of regional geochemical sampling, basic rocks were collected from the base, or the bit of the gravity corer was deformed by the base at eight points out of the total 39 points. Those eight points were located around the presumptive axial zone of the ridges. On the other hand, basic rocks were collected from the base, or the bit of the gravity corer was deformed by the base at 10 points out of the 14 points of the Base-line A (including uncollectable cases) and 14 points out of the 16 points of the Base-line B (including uncollectable cases) in the case of base-line geochemical sampling, which was carried out in the form of traversing the presumptive axial zone of the ridges.

Accordingly, information on base rocks was obtained from 32 points out of 69 points. But, the piercing capacity of the gravity corer is generally as low as a few centimeters. The highest one is 47cm, which was marked by R08 where brecciated basalt prevails. As a general result, only a few pieces of rock and that in the form of fragments were collected from base rocks. Basalt collected by the gravity corer is black hyaline, which is presumed to be the film part of the lava surface layer.

In the case of R03 by employing the power grab, small amounts of such subrounded pebbles as coral, coral limestone fragments, tuff and porphyrite were collected in addition to a large quantity of black vitric basalt. Photographs of basalt and coral limestone fragments obtained by the geochemical survey are shown in Figure 4-2-2-1 as typical rocks of this survey.

Of the rocks taken by the geochemical survey and ore deposit survey, 10 samples were selected for microscopical observation after making thin sections. And chemical analysis for major 13 elements was made for 10 pieces which were partly duplicated with just before mentioned 10 pieces for microscopical observation. The Table 4-2-2-1 shows the list of the specimens used for the two tests. The results of microscopical observation are shown in the Table 4-2-2-2 and the Figure 4-2-2-2 (1)~(4), while the results of the chemical analysis for 13 elements are shown in the Table 4-2-2-3. The details of the two tests are shown below.

1

2

1. Basalt (92RPG03)

2. Rock fragment of coral limestone (92RPG03)

Note: Each scale bar is 5 cm.

Figure 4-2-2-1 Photos of Substrates (Geochemical Investigation)

Table 4-2-2-1 List of Samples for Microscopic Observation and Chemical Analysis

No.	Sample No.	Depth(cm)	Method	Description
2	92RPG03-03		Chemical	back glassy basalt consist of bluish black glassy clinker part and black part including crack-shaped vesicle
3	92RPG03-04		Microscopic	
4	92RGC08-07	80	Chemical	black scoriaceous basalt with deposit of pale yellow clay in cracks or vesicle
5	92RGC10-06	172	Chemical	black glassy basalt including some phyrics of plagioclase
6	92RGC13-05	31~ 35	Chemical	black glassy basalt with no vesicle
8	92RGC27-03	29~ 43	Chemical	dark green dasite or dasitic tuff mainly consist of pale greenishgrey transparent volcanic glass with greenish grey clay mineral(chlorite)
9	92RGC27-04	29~ 43	Microscopic	
10	FDC04		Chemical	black vesicler grassy olivine basalt Phyrics of olivine is distinguishable.
11	FDC04		Microscopic	
13	92BGC02	79~105	Chemical	mainly black, partly pale brown~pale grey obsidian-like rock with stretched shape vesicles
14	92BGC02	79~105	Microscopic	
15	92BGC03	192~195	Microscopic	black glassy basalt
16	92BGC05	100~105	Microscopic	black vesicler glassy basalt
18	92HPG06		Chemical	black glassy~bluish grey vesicler basalt? or dasite? slightly devitrifidated
19	92HPG06		Microscopic	
27	92HPG14		Chemical	black vesicler glassy basalt
28	92HPG14		Microscopic	
32	92HPG19		Chemical	black vesicler glassy basalt
33	92HPG19		Microscopic	
37	92BGC20		Microscopic	black vesicler glassy basalt

Table 4-2-2-2 List of the Results of Microscopic Observation

No.	Sample No.	Rock Name	Rock Forming Mineral										Texture-structure	Remarks
			Phenocryst					Groundmass						
			Pl	Au	Hy	Ol	Fe	Pl	Au	Ol	Fe	Gl		
3	92RPG03-04	Non-porphyritic tholeiitic basalt						○	△	△		◎	Intersertal, quenching str.	Vesicular
9	92RGC27-04	Non-porphyritic dacite	△	+	+							◎	Felsic, glassy str., flow str.	A few alteration to chlorite
11	FDC04	Non-porphyritic augite-bearing olivine tholeiitic basalt	△	+		△		○	○		+	◎	Amygdaloidal, variolitic, quenching str.	Fairly bubbly, vesicular
14	92BGC02	Non-porphyritic glassy dacite (Rhyorite)										◎	Amygdaloidal, glassy str., flow str.	No minerals
15	92BGC03	Augite olivine alkali basalt	○	○		○		+	+	+		◎	Porphyritic, amygdaloidal, spherulitic, quenching str., glassy str.	Vesicular
16	92BGC05	Non-porphyritic alkali basalt	+					△	+	△		◎	Intersertal, variolitic, quenching str.	Vesicular
19	92HPG06	Non-porphyritic tholeiitic basalt	△	+			+	○	○		△	◎	Intersertal, quenching str.	
28	92HPG14	Non-porphyritic tholeiitic basalt	△	△				△	△			◎	Quenching str., glassy str.	Vesicular
33	92HPG19	Non-porphyritic tholeiitic basalt						○	△			◎	Variolitic, quenching str., flow str.	Vesicular
37	92BGC20	Olivine augite alkali basalt	○	◎		△		△	△	△		◎	Porphyritic, variolitic, quenching str.	

Notes) Pl : Plagioclase Au: Augite Hy: Hypersthene Ol : Olivine Fe : Fe-minerals
Gl : Glass

◎ : Abundant ○ : Common △ : Few + : Rare

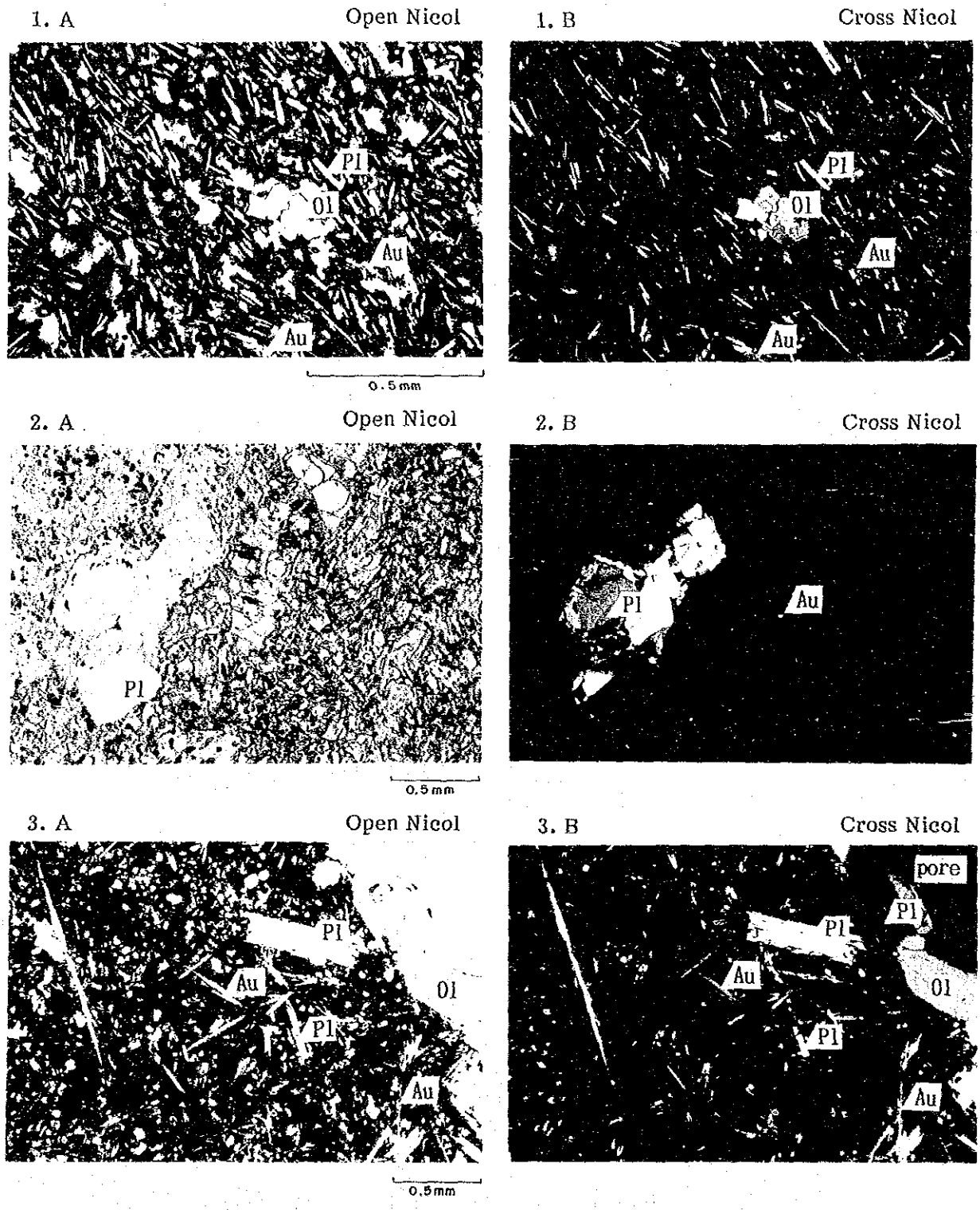

Notes Au: Augite, Ol: Olivine, Pl: Plagioclase, Pore: Vesicle

1. A. B: 92RPG03-04 Non-porphyritic Tholeiitic Basalt (×25)
2. A. B: 92RGC27-04 Non-porphyritic Dacite (×12.5)
3. A. B: FDC04 Non-porphyritic Augite-bearing Olivine Tholeiitic Basalt

Figure 4-2-2-2 Microscopic Photos of Rock (1)

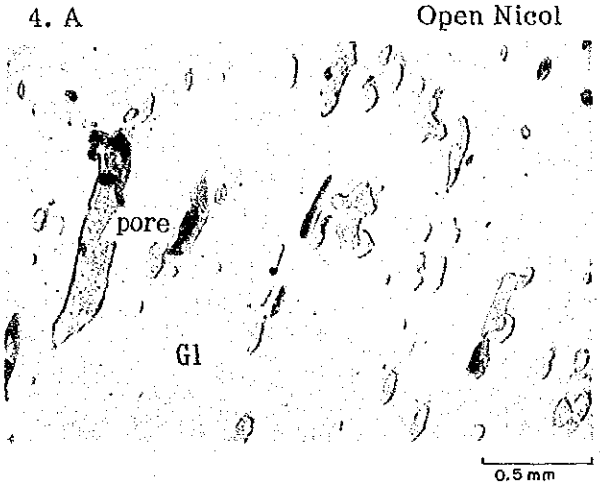

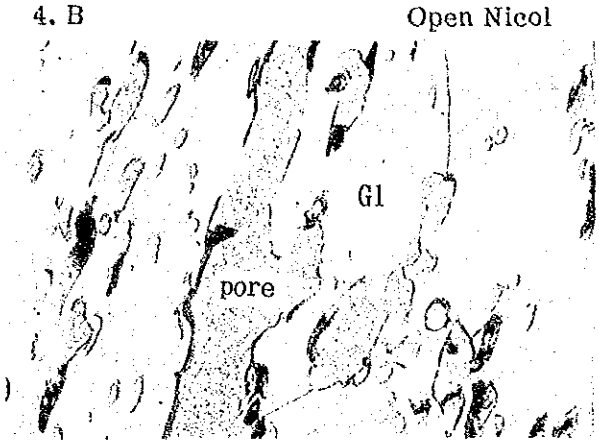

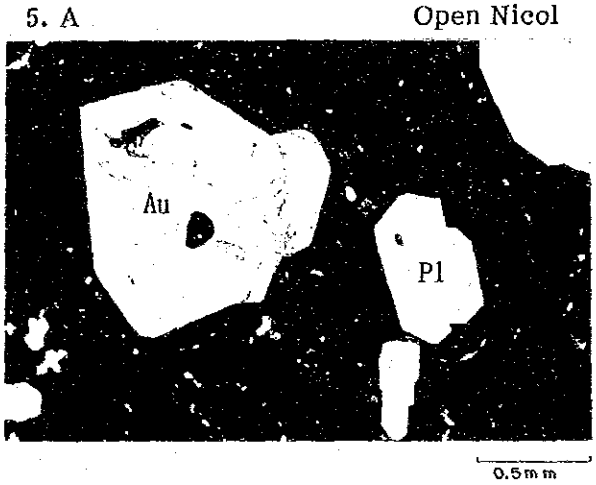

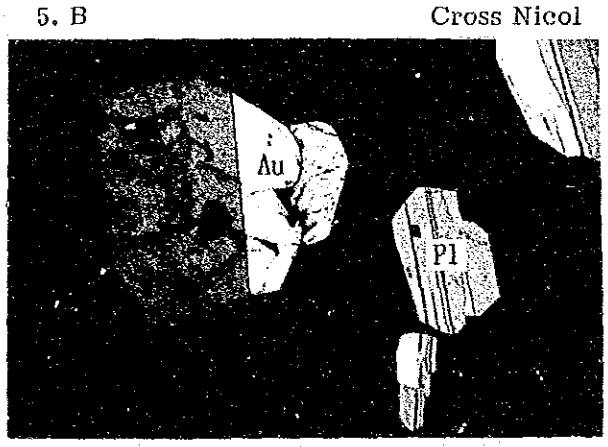

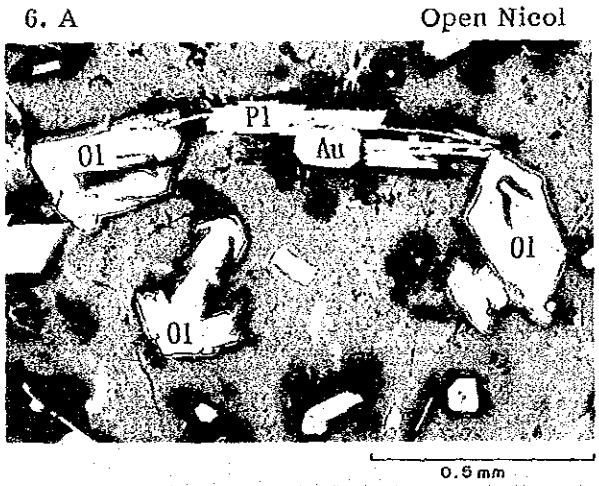

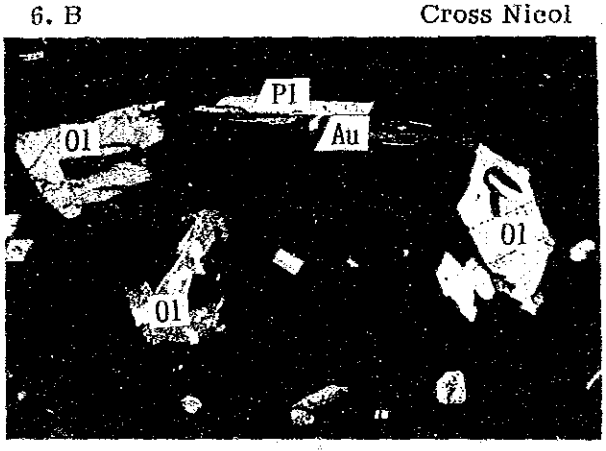

Notes Au: Augite, GL: Glass, Ol: Olivine, Pl: Plagioclase, Pore: Vesicle

4. A. B: 92BGC02 Non-porphyritic Glassy Dacite (Rhyolite) (×12.5)
5. A. B: 92BGC03 Augite Olivene Alkali Basalt (×12.5)
6. A. B: 92BGC05 Non-porphyritic Alkali Basalt (×25)

Figure 4-2-2-2 Microscopic Photos of Rock (2)

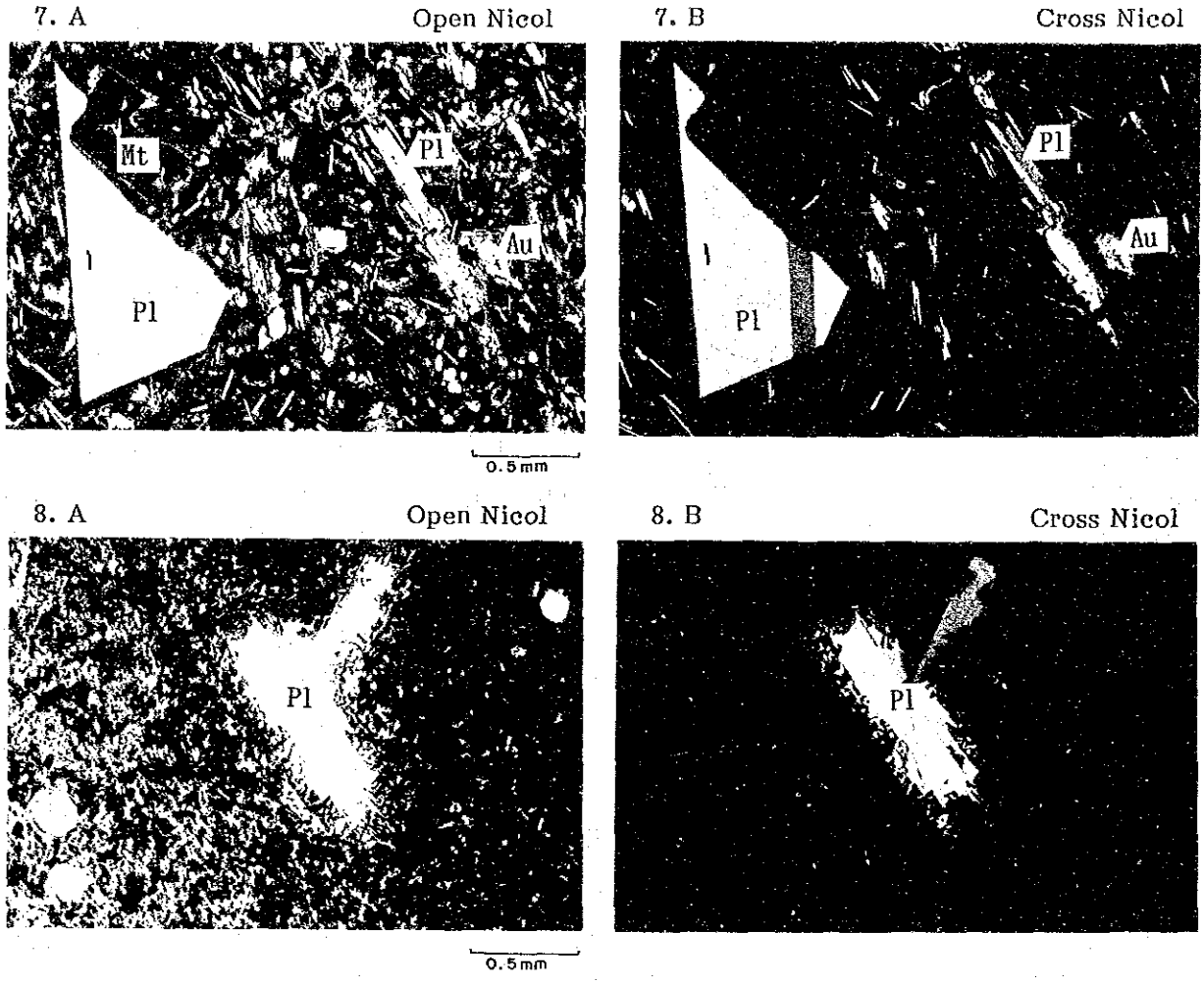

Notes Au: Augite, Mt: Magnetite, Pl: Plagioclase

7. A. B: 92HPG06 Non-porphyritic Tholeiitic Basalt (×12.5)
8. A. B: 92HPG14 Non-porphyritic Tholeiitic Basalt (×12.5)

Figure 4-2-2-2 Microscopic Photos of Rock (3)

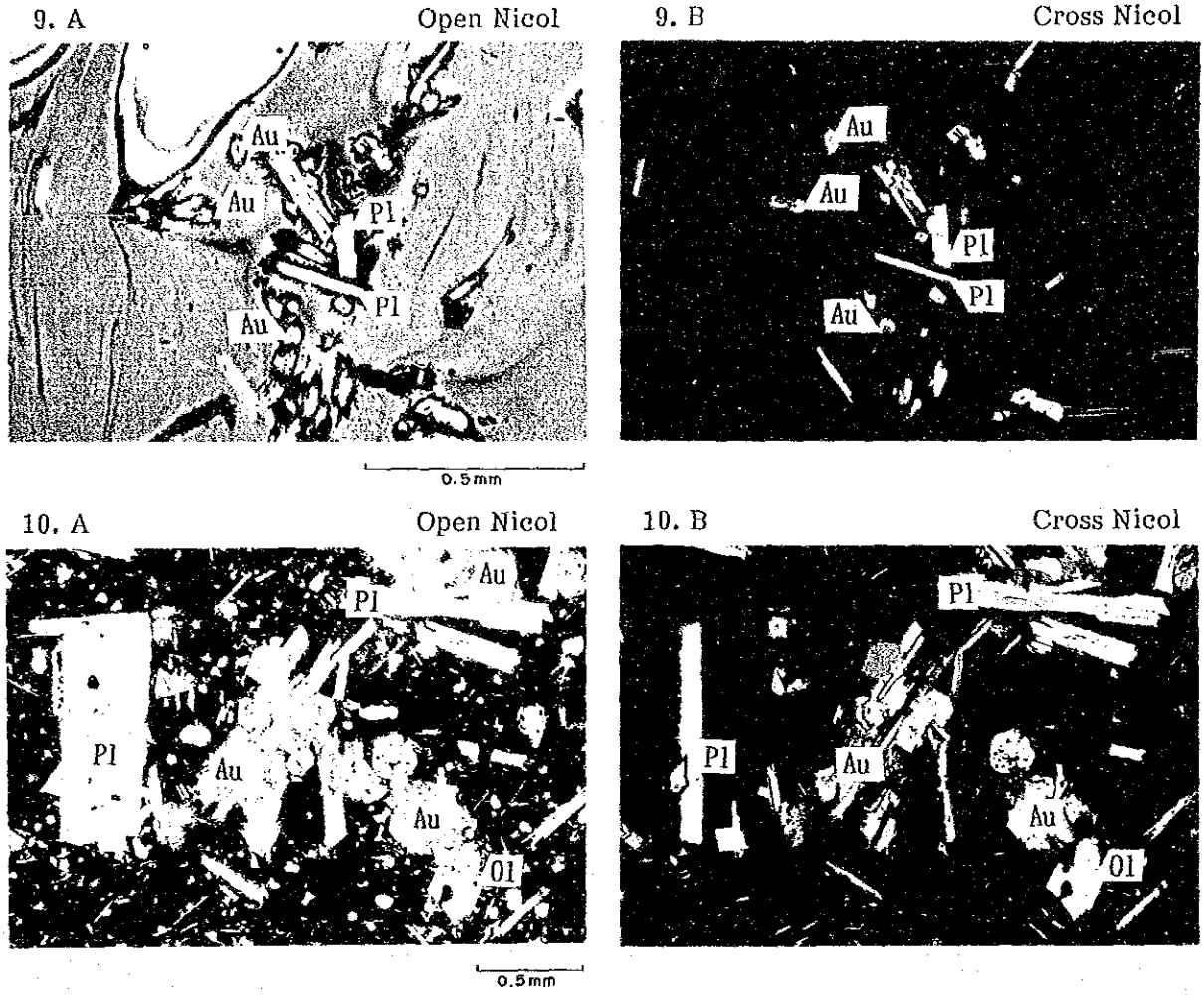

Notes Au: Augite, Ol: Olivine, Pl: Plagioclase

9. A. B : 92HPG19 Non-porphyritic Tholeiitic Basalt (×25)
10. A. B : 92BGC20 Olivine Augite Alkali Basalt (×12.5)

Figure 4-2-2-2 Microscopic Photos of Rock (4)

Table 4-2-2-3 Results of Chemical Analysis of Rock Samples

No.	Sample No.	SiO_2 %	TiO_2 %	Al_2O_3 %	Fe_2O_3 %	FeO %	MnO %	MgO %
1	92RPG03-03	53.71	1.98	14.13	3.91	8.37	0.21	3.81
2	92RGC08-07	24.55	3.27	15.21	15.32	0.73	0.23	7.77
3	92RGC10-06	49.22	1.78	14.71	2.41	8.71	0.19	5.81
4	92RGC13-05	50.28	3.87	12.38	4.06	11.03	0.21	4.46
5	92RGC27-03	65.94	0.26	11.07	2.21	1.95	0.05	0.66
6	92SFDC04	50.84	3.32	12.19	3.57	10.82	0.20	3.82
7	92BGC02	73.95	0.21	11.49	1.20	2.33	0.09	0.11
8	92HPG06	63.88	0.88	12.21	1.40	8.00	0.81	0.70
9	92HPG14	51.29	1.90	14.01	3.90	7.88	0.18	5.48
10	92HPG19	52.61	2.90	12.94	3.41	10.33	0.22	3.28

No.	Sample No.	CaO %	BaO %	Na_2O %	K_2O %	P_2O_5 %	LOI %	Total
1	92RPG03-03	7.66	0.029	3.67	0.71	0.44	1.31	99.94
2	92RGC08-07	4.08	0.048	2.78	0.29	0.74	21.80	96.83
3	92RGC10-06	11.44	0.024	2.82	0.55	0.19	1.93	99.76
4	92RGC13-05	8.59	0.035	3.02	0.73	0.88	0.97	100.53
5	92RGC27-03	1.37	0.048	3.52	3.55	0.03	9.54	100.20
6	92SFDC04	7.83	0.035	3.20	0.82	0.73	1.51	98.88
7	92BGC02	1.32	0.046	4.71	2.79	0.02	1.63	99.90
8	92HPG06	3.78	0.044	4.69	1.81	0.21	1.79	100.20
9	92HPG14	9.57	0.029	3.15	0.66	0.32	1.57	99.94
10	92HPG19	7.04	0.040	3.68	0.99	0.53	1.24	99.21

<Microscopical Observation for Thin Sections>

As a result of the observation, the 8 specimens were judged to be basalt and 2 specimens dacite (rhyolite). The details for each specimen are as follows.

[92RPG03-04]

Name of the rock: aphyric tholeiitic basalt

No phenocryst is seen at all, and plagioclase, augite, olivine and glass are seen as the groundmass.

The plagioclase is idiomorphic. Its size is smaller than 0.3mm and it exists commonly. The augite is hypidiomorphic, the size is smaller than 0.1mm, and a small amount is detected. The olivine shows xenomorphic, the size is smaller than 0.1mm, and a small amount is detected. Glass is detected in abundance.

It shows intersertal texture and a rapid-cooling texture. The pores created by bubbles are drawn long to the stream direction. It is porous.

[92RGC27-04]

Name of the rock: aphyric dacite

Plagioclase, augite and hypersthene are seen as phenocryst and glass is seen as groundmass.

The plagioclase shows hypidiomorph, the size being 1-0.1mm, and it occurs in small quantity (about 0.5% of the total weight). The augite and hypersthene are both micro-phenocryst rather than phenocryst, and they show also hypidiomorph. Their size is smaller than 0.1mm and they occur in trace (about 0.1%). Glass is seen in abundance.

It shows felsic texture, glassy texture and banding texture. The textures suggest the possibility that the rock reached the seafloor like a dome.

A slight alteration has received and chlorite has been produced.

[FDC04]

Name of the rock: aphyric augite olivine tholeiitic basalt

Plagioclase, augite and olivine are seen as phenocryst, and plagioclase, augite, iron minerals and glass are observed as groundmass.

The minerals of phenocrysts all show their idiomorph, and the size is 1-0.1mm. Quantity-wise, plagioclase>olivine>augite, but their total quantity is 2% at the most and they are largely aphyric.

The plagioclase in groundmass shows its idiomorph and occurs in medium amount. The augite shows hypidiomorph and occurs in medium amount. The iron minerals show their idiomorph and occur in trace. Glass is seen in abundance.

It shows amygdaloidal texture, variolitic texture and rapid-cooling texture. Vesicle texture are preserved in good condition and it is porous.

[92BGC02]

Name of the rock: aphyric glassy dacite (rhyolite)

No phenocryst is observed. Only glass is seen in abundance as groundmass.

It shows amygdaloidal texture, glassy texture and banding texture. Glass is porous, and gas pores are drawn along banding texture. No crystal is present due to rapid cooling.

[92BGC03]

Name of the rock: augite olivine alkali basalt

Plagioclase, augite and olivine are seen as phenocryst, and plagioclase, augite and glass are done as groundmass.

The minerals of phenocryst all show their idiomorph. Their sizes are 5-1mm, and they occur in a middle amount (10-15% as a whole).

The minerals in groundmass, except glass, show their idiomorph, and occur in trace. Glass is seen in abundance.

It shows porphyritic texture, amygdaloidal texture, spherulitic texture and rapid-cooling texture. It is porous.

[92BGC05]

Name of the rock: aphyric alkali basalt

Phenocryst consists of plagioclase, and groundmass consists of plagioclase, augite, olivine and glass.

The plagioclase of phenocryst presents its idiomorph, the size being 5-1mm, and occur in trace.

The minerals in the groundmass except glass represent their idiomorph, and their size is so small as microphenocryst ~ usual groundmass. They occur in small amount or trace. Glass is seen in abundance.

It shows intersertal texture, variolitic texture and rapid-cooling texture. It is porous.

[92HPG06]

Name of the rock: aphyric tholeiitic basalt

Phenocryst comprises plagioclase, augite and iron minerals, while groundmass comprises plagioclase, augite, iron minerals and glass.

The plagioclase of phenocryst represents its idiomorph, and occurs in trace (about 1%). Augite shows hypidiomorph, the size being 1-0.1mm, and it occurs in trace (less than 0.1%). The iron mineral (magnetite) shows hypidiomorph and occurs in trace.

All the minerals in groundmass except glass show their idiomorph, and are detected in medium to small amount. Glass is seen in abundance.

It shows intersertal texture and rapid-cooling texture.

[92HPG14]

Name of the rock: aphyric tholeiitic basalt

Plagioclase and augite are seen as phenocryst, while plagioclase, augite and glass are seen as groundmass.

The plagioclase of phenocryst shows its idiomorph, the size being 1-0.1mm, it occurs in small quantity. Augite shows hypidiomorph, its size ranges 1-0.1mm and it occurs in small quantity.

Plagioclase of groundmass shows its idiomorph and is recognized in small quantity. Augite represents hypidiomorph and is recognized in small quantity. Glass is seen in abundance.

It shows rapid-cooling texture and glassy texture, and is porous.

[92HPG19]

Name of the rock: aphyric tholeiitic basalt

No phenocryst is recognized at all. Plagioclase, augite and glass are recognized as groundmass.

Plagioclase represents its idiomorph and is found in medium quantity. Augite shows hypidiomorph and is seen in small amount. Glass is seen in large quantity.

It shows variolitic texture, rapid-cooling texture and banding texture, and is porous.

[92BGC20]

Name of the rock: olivine augite alkali basalt

Phenocryst comprises plagioclase, augite and olivine, while groundmass contains plagioclase, augite, olivine and glass.

All the minerals in phenocryst represent their idiomorph, and the size varies 1-0.1mm. Quantity-wise, they occur in the order of augite (large amount) > plagioclase(medium quantity) > olivine (small amount).

All the minerals in groundmass, except glass show hypidiomorph and occur in small quantities. Glass is recognized in large quantity.

It shows porphyritic texture, variolitic texture and rapid-cooling texture.

<Complete analysis of rocks>

The analized components and the mimimum detectible values are as follows:

SiO_2, TiO_2, Al_2O_3, Fe_2O_3, FeO, MnO, MgO, CaO, BaO, Na_2O, K_2O, P_2O_5, LOI (The analysis limit for these 13 components is 0.01%.)

Analytical method is summarized in Table 4-2-2-4, and maximum, minimum and average value of analized components are shown in Table 4-2-2-5.

Most of the specimens of the volcanic rocks which were analyzed show rather weak alteration, and the analyzed values are thought to represent almost initial values of the specimens. The specimen 92RGC08-07, however, has a large LOI value, being 21.81% and the sum of analyzed values add up to a little less than 98%, which means that it has obviously gone through a strong secondary alteration.

Judging from the SiO2 value and the alkali contents (Na_2O+K_2O), the specimens are deemed to range widely from basaltic and rhyolitic. The rock types of each specimen as estimated from the analysis are as follows:

Specimen No.	Rock types
92RPG03-03	basaltic andesite
92RGC08-07	(undefinable due to alteration)
92RGC10-06	basalt
92RGC13-05	basalt
92RGC27-03	dacitic rock
92SFDC04	basalt
92BGC02	rhyolite
92HPG06	dacite
92HPG14	basalt
92HPG19	basaltic andesite

Basaltic rocks in these specimens are rich in P_2O_5 (0.19~0.89%) and TiO_2 (1.78~3.87%), and they have a general character as oceanic basalt.

Table 4-2-2-4 Method of Chemical Analysis of Rock Samples for Major 13 Elements

Method	Elements
X-ray Fluorescent Analysis	SiO_2, TiO_2, Al_2O_3, Fe_2O_3, MnO, MgO, CaO, Na_2O, K_2O, P_2O_5, BaO
Titration	FeO
Ignition Loss	LOI

*Crushing: Using a ring mill made by chromium steel, the specimen is crushed so that more than 90% of the sample may pass the 150 mesh.

*Fluorescent X-ray analysis: After determining the red-heat loss, about 1.0 gram of the powdered specimen is put into a crucible of 95% Pt and 5% Au. 4 boric acid lithium of 4 times the quantity of the specimen and about 0.003g of lithium

bromide are added into the same crucible and heated to produce glassy bead. An Rh tube is attached to the fluorescent X-ray analyzer (made by Rigaku Corp. 3080E2), and the specimens were analyzed at 45kv, 40mA (in the case of Ba tube, 50kv, 50mA). In order to construct a calibration curve, we have used the standard specimens of the volcanic rock series prepared by Geological Survey in Japan and GIT-IWGś MA-N, and also we have used standard compound which we had made ourselves by adding pure reagents to them and natural rock samples whose wet analysis values are already available. Total number of standard samples is 43.

*Titration: 0.2g of the powdered specimen is dissolved into hydrochloric acid-fluoric acid. The solution is neutralized by adding boric acid. The solution is cooled down to the room temperature and is titrated with potassium permanganate.

*Quantity reduction in intense heat: A magnetic crucible is dried in an oven at 105oC and weighed after natural cooling. 1.00g of the powdered specimen is taken into a crucible and is red-heated for one hour at 1000oC. It is then weighed after cooling it naturally in a decicater and weight loss of the specimen is calculated.

Table 4-2-2-5 Maximum, Minimum and Average Values of Rocks Analysis

Element	Max. (%)	Min. (%)	Average (%)	Element	Max. (%)	Min. (%)	Average (%)
SiO_2	73.95	24.55	53.63	CaO	11.44	1.32	6.27
TiO_2	3.87	0.21	2.04	BaO	0.048	0.024	0.038
Al_2O_3	15.21	11.07	13.03	Na_2O	4.71	2.78	3.52
Fe_2O_3	15.32	1.20	4.14	K_2O	3.55	0.29	1.29
FeO	11.03	0.73	7.02	P_2O_5	0.88	0.02	0.41
MnO	0.81	0.05	0.24	LOI	21.80	0.97	4.33
MgO	7.77	0.11	3.59	Total	100.53	96.83	99.54

3) Others

As revealed by the FDC survey, pieces of wood are often recognized on the sea-floor of these waters. Pieces of wood of about 1 cm size were universally recognized, though a small quantity, in the muddy substances sampled from the geochemical survey. A "wooden bed" buried between the depth of 83~88 cm was found in the sample R35.

In order to determine the accumulation speed of sediments, we have determined the age of this "wood piece" by the carbon 14 method. The specimen is soft enough to be deformed simply by pressing with fingers, and does not retain its original shape. The color tone is yellow-brownish to dark-brownish, and retains a fiber form of a tree-trunk. As a result of measurement, the age of this wood shows 4,350+/-240 year BP, and the average accumulation speed of the upper sediments proved to be 195mm/1000 years. The details of the measurement are described below.

<Age determination by C^{14} method>

① Procedure of measurement

(1) Preparation of the specimen

The specimen is washed in water after it has been heated in HC1 of 1N for 60 minutes, and then dried.

(2) Recovery of carbon

It is heated and burnt in air stream where CO_2 has been removed. Oxygen is added to it and it is then passed through heated oxide copper so that carbon will become CO_2. And this is then absorbed into ammonia water of 6N, to which $CaCl_2$ solution is added so that $CaCO_3$ will precipitate from the heated solution. Thus, carbon is recovered.

(3) Composing acetylene gas

Lithium metal placed inside the stainless tube is heated up to 400-600°C and cause reaction to CO_2 which has been generated by reaction between $CaCO_3$ and perchlorine, so that Li_2C_2 will be composed.

$$2CO_2 + 10Li \rightarrow 4Li_2 + Li_2C_2 + 2O_2 \uparrow$$

Then, water is added into the stainless tube, inside of which Li_2C_2 has been formed, so that acetylene (C_2H_2) will be formed.

$$Li_2C_2 + H_2O \rightarrow Li_2O + C_2H_2$$

(4) Computation of Beta Lines

Acetylene gas is contained in a proportional counting tube, and the counted figures are totalized every one hour while controling by a computer. The beta line counted rate (cpm) is thus calculated.

(5) Calcuration of the age value

The age value (t) is obtained by the following formula from the cpm (=No) of acetylene gas which has been made with the present standard carbon (Modern std.) and the sample acetylene gas measurement (cpm=N) under the same temperature and pressure.

$$T = \frac{T\ 1/2}{0.693} \log_e \left(\frac{No}{N}\right)$$

T 1/2 (a half life) = 5,570 years

② Measurement results

The results of the measurement by the above method are as follows:

4,350 ± 240 years BP

The amount of carbon extracted from the specimen is so small that there is such a large error in the age.

4-3 Survey Results

1) Chemical Analysis

We have made chemical analysis on 250 samples of sea-floor sediments taken in the area. The Appendix 4 shows the list of the samples for the analysis. The chemical components and their minimum detectible contents are as follows:

SiO_2, TiO_2, Al_2O_3, Fe_2O_3, FeO, MnO, MgO, CaO, BaO, Na_2O, K_2O, P_2O_5, LOI (their minimum detectible contents are 0.01% each), Ag (0.02ppm), Ni (1ppm), Cu (0.2ppm), Co (1ppm), Pb (0.5ppm), Zn (1ppm), Mn (5ppm), Cd (0.1ppm), As (0.2ppm), Sb (0.2ppm), Mo (0.2ppm), Ga (1ppm), Sr (1ppm), Hg (10ppb), Ba (5ppm), Au (5ppb), S (0.001%), P (0.005%), Cl (100ppm), T-R_2O_3 (1ppm)

The analysis procedure for each component is shown in the Table 4-3-1-1. Of the analysis resutls, the analysis for the 13 major components is shown in the Appendix 6 while the Appendix 7 shows the analysis for 20 trace elements.

Table 4-3-1-1 Method of Chemical Analysis of Sediments for 33 Elements

Method	Elements
Inductively Coupled Plasma Emission Spectrum (1)	SiO_2, TiO_2, Al_2O_3, Fe_2O_3, MnO, MgO, CaO, Na_2O, K_2O, P_2O_5, P
Inductively Coupled Plasma Emission Spectrum (2)	BaO, Ba, Ni, Co, Mn, Cd, Sr
Inductively Coupled Plasma Emission Spectrum (3)	Ag, Cu, Pb, Zn, As, Sb, Mo, Ga
Neutron Activation Analysis	T-R_2O_3, Cl
Dry-Atomic Absorption Analysis	Au
Flameless Atomic Absorption Analysis	Hg
Infrared Absorption Analysis	S
Titration	FeO
Gravimetric Analysis	LOI

The details of analytical method are left out here, because they are normal methods.

Table 4-3-2-1 Measuring Condition of X-ray Diffraction Analysis

Items	Measurement Condition	
	Random Orientation Method	Hydrauric Elutriation Method, EG-HCL Treatment
X-ray Diffractmeter	RIGAKU Corp. Geiger Flex	RIGAKU Corp. Geiger Flex
Anticathode	Cu	Cu
Filter	Ni	Ni
Tube Voltage	30 kV	30 kV
Tube Electoric Current	15 mA	15 mA
Count Full Scale	1,000 cps	1,000 cps
Constant Time	1 sec	1 sec
Chart Speed	4 cm/ min	4 cm/ min
Scanning Speed	4° / min	2° / min
Slit System	1° - 0.3mm - 1°	1° - 0.3mm - 1°
Scanning Range	2θ = 2~70°	2θ = 2~20°

Table 4-3-2-2 Results of X-ray Diffraction Analysis (1)

			Silicate Minerals													Sulfate Minerals		Carbonate Minerals		Other Minerals				Remarks	Treatment	
			Silica		Feldspar			Zeolite			Clay Minerals																
No.	Sample No.	Depth (cm)	Quartz	Cristobalite	Plagioclase	Albite	Potash Feldspar	Analcite	Heulandite	Phillipsite	Chlorite	Sericite	S/M	Montmorillonite		Gypsum		Calcite	Aragonite	Pyrite	Iron Hydroxide	Halite	Amorphous Silica		EG	HCl
1	92RLC01-01	0～ 5	+		△			+			+		+	△		+		○	+						*	
2	92RLC01-02	11～ 16	+		○			+	+		+		+	+				○	+			△			*	*
3	92RLC01-03	26～ 31	+		+						+	+						◎				△				
4	92RLC01-04	75～ 80	+		+						+			+				◎	+			○				
5	92RLC01-05	165～170	+		○						+							○	+			△				
6	92RLC01-06	292～297	△		+						+		+					◎		+		○				
7	92ROG02		+		+			+				+				+		◎	+			△				
8	92RPG03-01	0～ 5	+		△			+			+		+					○	+			△			*	*
9	92RPG03-02	10～ 15	+			○		+	+		+		+	△				○	+			△			*	*
10	92RLC04-01	0～ 5	+		△			+			+		+			+		◎				○			*	
11	92RLC04-02	15～ 20	+		△			+			+		+	△		+		○	+			△			*	*
12	92RLC04-03	45～ 50	+		+						?			+				◎	+			△				
13	92RLC04-04	147～152	+		+						+	+		+				◎		+		○			*	*
14	92RLC04-05	222～227	+		+						+	+		+				○	+			○			*	*
15	92RPG05-01	0～ 5	+		+			+			+	+		+				◎				△			*	
16	92RPG05-02	43～ 48	+		△				+		+	+		+				◎	△			△			*	
17	92RPG06-01	0～ 5	+		+						+	+		+				◎				△			*	*
18	92RPG06-02	13～ 18	+		+		?		+		+			+				◎				△				
19	92RPG06-03	37～ 42	+		+						+			+				○	+			○			*	
20	92RGC07-01	0～ 5	+		+			+			+			+				◎	△			△				
21	92RGC07-02	15～ 20			+									+		+		◎	△			△				
22	92RGC07-03	92～ 97	+		+						+	+	+					◎				△				
23	92RGC07-04	151～154	+		+						+	+		+				○				△			*	
24	92RGC07-05	172～177	○		○				+	?	+		+					○	△			△			*	*
25	92RGC08-01	0～ 5	+		◎									+				○	△			+				
26	92RGC08-02	15～ 20	△		+						+			+				◎	○			△				
27	92RGC08-03	45～ 50	+		○													○	○			△				
28	92RGC08-04	60～ 65	+		△						+							○	△			+				
29	92RGC08-05	80～ 85	+		△											+		○	△							
30	92RGC08-06	130～135			○																					
31	92RGC09-01	0～ 5	△		△						+	+	+			+		◎				△			*	*
32	92RGC09-02	13～ 18	△		+						+	+		+		+		◎				△			*	*
33	92RGC09-03	65～ 70	△		△						+	+		+		+		◎				△			*	*
34	92RGC09-04	120～125	△		△						+	+	+					◎				△			*	*
35	92RGC10-01	0～ 5	+		○		+	+	+		+	+	+			+		△				+			*	*
36	92RGC10-02	16～ 20	△		+						+	+	+			+		○				△				*
37	92RGC10-03	25～ 30	+		△				+		+	+	+			+		○				△	+			
38	92RGC10-04	70～ 75	△		+			+			+	+		+		+		◎				△			*	*
39	92RGC10-05	165～170	△		△						+	+		+		+		◎				△			*	*
40	92RGC11-01	0～ 5	△		◎									+		+		○				△			*	

◎:Strong ○:Middle △:Weak +:Very Weak ?:Indistinct

S/M:Mixedlayered Clay Mineral of Sericite-Montmorillonite

Table 4-3-2-2 Results of X-ray Diffraction Analysis (2)

No.	Sample No.	Depth (cm)	Silicate Minerals: Silica: Quartz	Silica: Cristobalite	Feldspar: Plagioclase	Feldspar: Albite	Feldspar: Potash Feldspar	Zeolite: Analcite	Zeolite: Heulandite	Zeolite: Phillipsite	Clay Minerals: Chlorite	Clay Minerals: Sericite	Clay Minerals: S/M	Clay Minerals: Montmorillonite	Sulfate Minerals: Gypsum	Sulfate Minerals:	Carbonate Minerals: Calcite	Carbonate Minerals: Aragonite	Other Minerals: Pyrite	Other Minerals: Iron Hydroxide	Other Minerals: Halite	Other Minerals: Amorphous Silica	Remarks	Treatment: EG	Treatment: HCl
41	92RGC11-02	10～ 15	△		○			+	+		+	+	+		+		△				+			*	*
42	92RGC11-03	30～ 35	△		△			+	+		+	+	+	+	+		△				+			*	*
43	92RGC11-04	55～ 60	+		○		+	+	+		+	+	+				△				△			*	*
44	92RGC11-05	64～ 68	○		△			+	+		+	+	+				○		+		△			*	*
45	92RGC11-06	115～120	+		△			+	+		+	+	+				△		+		+			*	*
46	92RGC11-07	152～157	○		+						+	+		+	+		◎				+				*
47	92RGC11-08	195～200	+		○		+	+	+		+	+	+	△	+		○				△			*	
48	92RGC12-01	0～ 5	+		+						+	+	+		+		◎				△				
49	92RGC12-02	15～ 20	+		+						+	+	+				◎				+				
50	92RGC12-03	35～ 40	+		+						+			+			◎	+			△			*	*
51	92RGC12-04	85～ 90	+		△						+		+				○	+			△				
52	92RGC12-05	140～145	+		+						+			+			◎	+			△				
53	92RGC13-01	0～ 5	△		△			+	+		+	+	+				○				△			*	
54	92RGC13-02	10～ 15	+		○			+	+		+			+			△				+			*	*
55	92RGC13-03	20～ 25	△		△		+				+			+			◎				△				*
56	92RGC13-04	27～ 41	△		△						+	+	+				○				△				
57	92RGC14-01	0～ 5	△		△						+	+					◎				△				
58	92RGC14-02	20～ 25	+		△						+	+					○				△				
59	92RGC14-03	36～ 39	△		△						+			+			◎				△				
60	92RGC14-04	43～ 46	+		△									+			△				△	△			
61	92RGC14-05	46～ 51	+		△						+	+	+				○		+		+				
62	92RGC14-06	70～ 75	+		+						+	+	+				◎		+		△				
63	92RGC14-07	140～145	+		+						+	+	+				◎		+		+			*	*
64	92ROG15-01	0～ 8	+	△	△			+			+	+					◎				△				
65	92ROG15-02	8～ 20	+		△			+			+	+			+		◎				△				*
66	92RGC16-01	0～ 5	△		○			+			+	+					○				○				
67	92RGC16-02	10～ 15	△		+						+	+	+				◎				△				
68	92RGC16-03	17～ 21	△		+						+	+	+				◎				△			*	*
69	92RGC16-04	31～ 34	+		○						+	+					○				△	△			
70	92RGC16-05	34～ 38	△		△						+	+	+				○				△			*	
71	92RGC16-06	50～ 55	+		+						+	+		+			◎		+		△			*	*
72	92RGC16-07	185～180	+		+						+	+		+			◎		+		+			*	*
73	92RGC17-01	0～ 5	△		+			+	+		+	+	+				◎				△			*	
74	92RGC17-02	8～ 13	+		△			+			+	+	+				○				△			*	*
75	92RGC17-03	20～ 25	△		+						+	+		+			◎				△			*	*
76	92RGC17-04	35～ 40	+		△									+			△				+	△			
77	92ROG18-01	0～ 5	+		+						+	+					◎				△				
78	92ROG18-02	22～ 27	+		+				+		+	+					◎				△				
79	92RGC19-01	0～ 5	△		△						+	+			+		◎	+			△				
80	92RGC19-02	20～ 25	△		△			+			+	+	+				○				△			*	*

◎:Strong ○:Middle △:Weak +:Very Weak ?:Indistinct

S/M:Mixedlayered Clay Mineral of Sericite-Montmorillonite

Table 4-3-2-2 Results of X-ray Diffraction Analysis (3)

			Silicate Minerals												Sulfate Minerals		Carbonate Minerals		Other Minerals				Remarks	Treatment	
			Silica		Feldspar			Zeolite			Clay Minerals													EG	HCl
No.	Sample No.	Depth(cm)	Quartz	Cristobalite	Plagioclase	Albite	Potash Feldspar	Analcite	Heulandite	Phillipsite	Chlorite	Sericite	S/M	Montmorillonite	Gypsum		Calcite	Aragonite	Pyrite	Iron Hydroxide	Halite	Amorphous Silica			
81	92RGC19-03	50～ 55	△		+						+	+	+				◎	?			+			*	*
82	92RGC19-04	185～190	△		+						+	+	+				◎	+			△			*	*
83	92RGC20-01	0～ 5	+		+						+	+	+				◎	△			△				
84	92RGC20-02	20～ 25	+		+						+	+					◎	△			△				
85	92RGC20-03	195～200	+		+						+			+			◎	+			△				
86	92RGC21-01	0～ 5	+		+						+	+					◎	+			△				
87	92RGC21-02	11～ 16	△		+						+	+					◎	+			△				
88	92RGC21-03	40～ 45	+		+						+	+					◎	△			△				
89	92RGC21-04	205～210	+		+						+	+	+				◎	△			△			*	*
90	92RGC22-01	0～ 5	△		△			+			+	+	+				◎				○			*	*
91	92RGC22-02	15～ 20	○		○						+	+	+				○				△			*	*
92	92RGC22-03	35～ 40	△		△						+	+	+				○		+		△			*	*
93	92RGC22-04	171～176	+		○						+	+	+				△		+		+				
94	92RGC23-01	0～ 5	△		+						+	+	+	+			◎				○			*	*
95	92RGC23-02	20～ 25	△		△						+	+	+				◎				△			*	*
96	92RGC23-03	40～ 45	△		+						+	+	+				◎				△			*	*
97	92RGC23-04	180～185	○		+						+	+	+				◎		+		△			*	*
98	92RGC24-01	0～ 5	+		+						+	+	+				◎		+		○			*	*
99	92RGC24-02	15～ 20	+		+						+	+	+				◎	+			○			*	*
100	92RGC24-03	23～ 29	+		○			+			+	+	+				◎				△			*	*
101	92RGC24-04	29～ 35	+		+			+			+	+					◎				△				*
102	92RGC24-05	45～ 50	+		+						+	+		+			◎	+			△			*	*
103	92RGC24-06	185～190	△		+						+	+	+				◎	+			△			*	*
104	92RGC25-01	0～ 5	+		+						+						◎	△			○				
105	92RGC25-02	30～ 35	+		○				+		+						○	△			△				
106	92RGC25-03	35～ 40	+		+						+		+				◎	○			△				
107	92RGC25-04	40～ 45	+		+				+		+	+					◎	△			△				
108	92RGC25-05	135～140	+		+						+	+					◎	△			△				
109	92RGC26-01	0～ 5	+		+						+	+	+				◎	+			△			*	
110	92RGC26-02	7～ 12	+		+						+	+					◎	+			△				
111	92RGC26-03	15～ 19	+		+					+	+			+			◎	+			△				
112	92RGC26-04	19～ 24	+		+				+		+			+			◎	+			△				
113	92RGC26-05	25～ 30	+		+						+	+		+			◎	+			△			*	
114	92RGC26-06	85～ 90	+		△						+	+					◎	+			△				
115	92RGC26-07	138～141	+		+						+			+			◎	+			△			*	
116	92RGC27-01	0～ 5	+		+						+						◎	△			△				
117	92RGC27-02	10～ 15	+		+									+			◎	+			△				
118	92HPG04																+			※	+				
119	92RGC28-01	0～ 5	◎			△		+			△	+		+			+				+			*	*
120	92RGC28-02	33～ 39	◎			△			+	+	△	+		+			+				△			*	*

◎:Strong ○:Middle △:Weak +:Very Weak ?:Indistinct

S/M:Mixedlayered Clay Mineral of Sericite-Montmorillonite

※:Amorphous Iron Oxide or Hydroxide?

Table 4-3-2-2 Results of X-ray Diffraction Analysis (4)

No.	Sample No.	Depth(cm)	Silicate Minerals: Silica: Quartz	Silica: Cristobalite	Feldspar: Plagioclase	Feldspar: Albite	Feldspar: Potash Feldspar	Zeolite: Analcite	Zeolite: Heulandite	Zeolite: Phillipsite	Clay Minerals: Chlorite	Clay Minerals: Sericite	Clay Minerals: S/M	Clay Minerals: Montmorillonite	Sulfate Minerals: Gypsum	Sulfate Minerals:	Carbonate Minerals: Calcite	Carbonate Minerals: Aragonite	Other Minerals: Pyrite	Other Minerals: Iron Hydroxide	Other Minerals: Halite	Other Minerals: Amorphous Silica	Remarks	Treatment: EG	Treatment: HCl
123	92RGC29-01	0～ 5	+		+							+	+	+			◎				△				
124	92RGC29-02	5～ 10	+		△									+			◎				△				
127	92BGC01-01	0～ 5	+		+									+			◎	+			△				
128	92BGC01-02	7～ 15	+		△						+		+				◎	+			△				
133	92BGC02-01	0～ 5	+		+						+		+				◎	+			△				
134	92BGC02-02	25～ 30	+		△						+						◎	+			△				
138	92BGC03-01	0～ 5	+		+						+	+					○				△				
139	92BGC03-02	10～ 15	+		+						+	+					○	+			△				
145	92BGC04-01	0～ 5	+		+						+			+			◎				○				
146	92BGC04-02	22～ 29	+		+						+			+			◎				△				
148	92BGC05-01	0～ 5	+		△									+	+		○				△				
149	92BGC05-02	15～ 20	+		+						+			+			◎				△				
154	92BGC07-01	0～ 5	+		△			+			+			+			○				△				
155	92BGC07-02	10～ 15	+		+									+	+		◎				△				
156	92BGC08	0～ 2	+		+						+	+					◎				△				
157	92BGC09-01	0～ 4	+		+						+		+				◎				△				
158	92BGC09-02	5～ 10	+		+						+			+			○				△				
159	92BOG11		+		+												+				+				
160	92BPG12-01	0～ 5	+		△						+						◎				△				
161	92BPG12-02	15～ 20	+		+									+	+		◎				△				
162	92BOG13-01	0～ 5	+		+			+			+		+				◎				△				
163	92BOG13-02	15～ 20	+		+						+	+	+				◎				△				
164	92BGC14-01	0～ 5	+		+						+						○				△				
165	92BGC14-02	8～ 13	+		+												△				+				
166	92BGC15-01	0～ 5	+		+			+						+			◎				△				
167	92BGC15-02	7～ 13	+		+						+			+			◎				△				
172	92BGC16-01	0～ 5	+		△						+			+			◎	+			△				
174	92BGC16-03	70～ 75	+		+						+			+			◎	+			△				
177	92HPG07-01																			※	△				
180	92HPG10-01		+		+									+			○				△				
186	92HPG15-01		+									+		△							+				*
188	92HPG15-03		+		+							+		+						※	+				
189	92HOG16		+		+			+			+	+					△				△				
193	92HOG22		+		+			+	+		+						○				△				
195	92HOG24		+		△			+			+	+					○				△				
197	92BGC17-01	0～ 4	+		△										+		○				+				
198	92BGC17-02	4～ 8	+		△						+	+					○				△				
202	92BGC18-01	0～ 5	+		+						+	+					◎				△				
203	92BGC18-02	10～ 15	+		+						+	+			+		◎				△				
206	92BGC19-01	0～ 5	+		+						+	+			+		◎				△				

◎:Strong ○:Middle △:Weak +:Very Weak ?:Indistinct

S/M:Mixedlayered Clay Mineral of Sericite-Montmorillonite

※:Amorphous Iron Oxide or Hydroxide?

Table 4-3-2-2 Results of X-ray Diffraction Analysis (5)

No.	Sample No.	Depth(cm)	Silicate Minerals: Silica: Quartz	Silica: Cristobalite	Feldspar: Plagioclase	Feldspar: Albite	Feldspar: Potash Feldspar	Zeolite: Analcite	Zeolite: Heulandite	Zeolite: Phillipsite	Clay Minerals: Chlorite	Clay Minerals: Sericite	Clay Minerals: S/M	Clay Minerals: Montmorillonite	Sulfate Minerals: Gypsum	Sulfate Minerals:	Carbonate Minerals: Calcite	Carbonate Minerals: Aragonite	Other Minerals: Pyrite	Other Minerals: Iron Hydroxide	Other Minerals: Halite	Other Minerals: Amorphous Silica	Remarks	Treatment: EG	Treatment: HCl
207	92BGC19-02	10～15	△		△			+			+	+					○				△			*	*
209	92BGC20-01	0～5	△		△			+			+	+	+				○				△			*	*
210	92BGC20-02	5～10	△		+			+			+	+	+				○				△			*	*
213	92BGC21-01	0～5	+		△			+			+	+		+			○				△			*	*
214	92BGC21-02	24～28	+		△						+						○		+		△	+			
217	92BGC22-01	0～5	+		△			+			+				+		○				△				
218	92BGC22-02	21～29			○												+				△				
221	92BGC24-01	0～5	△		+						+	+					◎				△				
222	92BGC25-01	2～8	+		+						+	+					○				△				
226	92BGC26-01	0～4	+		○			+	+		+	+			+		○				△				
227	92BGC27-01	0～5	+		△						+	+	+				○				△			*	*
228	92BGC27-02	20～25	+		+				+		+	+	+				◎				△			*	*
231	92BGC28-01	0～5	+		△		+	+	+		+	+	+				○				△			*	*
232	92BGC28-02	15～20	+		△		+	+	+		+	+	+		+		○				△			*	*
235	92BGC29-01	0～5	+		+						+	+					◎				△				
236	92BGC29-02	16～20	+		+						+	+					○	?			△				
239	92BGC30-01	0～5	+		△			+	+		+	+		+			○				△				
240	92BGC30-02	15～20	+		△						+	+					○				+	+		*	*
242	92RGC30-01	0～5	+		+			+			+	+	+				◎				△			*	*
243	92RGC30-02	10～15	+		△			+			+	+	+				△				+			*	*
246	92RGC31-01	0～5	○		△						+	+	+				○				△			*	*
247	92RGC31-02	23～27	△		△			+	+		+	+	+				△				△			*	*
251	92RGC32-01	0～5	○		△				+	+	△	+	+				+				△			*	*
252	92RGC32-02	10～15	○		○				+	+	△	+	+								+			*	*
254	92RGC33-01	0～5	+		+					+	+	+	+				◎				○			*	*
255	92RGC33-02	8～13	△		+			+			+	+	+				○				△			*	*
258	92RGC34-01	0～5	○		△				+	+	+	+	+				○	+			△			*	*
259	92RGC34-02	16～23	○		△			+	+		+	+	+				△				+				*
262	92RGC35-01	0～5	○		△			?	+	+	+	+	+				△				+				*
263	92RGC35-02	14～20	○		△			+	+	+	+	+	+				○				△			*	*
266	92RGC36-01	0～5	◎		○				+	+	△	△	+								△			*	*
268	92RGC36-03	55～60	◎		○				+	△	○	△		+							+			*	*
269	92RGC37-01	0～5	○			△			+	+	△	+	+				+				+			*	*
270	92RGC37-02	15～20	◎			○		+	+	+	△	+	+				+				+			*	*
273	92RGC38-01	0～5	○			△		+	+	+	△	+	+				+				△			*	*
274	92RGC38-02	16～21	◎			○			+	+	○	△	+						+		+			*	*
277	92RGC39-01	0～5	○		+						+	+	+				○				○			*	*
278	92RGC39-02	20～25	○		+						+	+	+				○				△			*	*
279	92HPG07-02																			※	+				
280	92HPG19				+									+								+			

◎:Strong ○:Middle △:Weak +:Very Weak ?:Indistinct

S/M:Mixedlayered Clay Mineral of Sericite-Montmorillonite

※:Amorphous Iron Oxide or Hydroxide?

2) X-ray Diffraction

The samples tested for X-ray diffraction were 200 specimens of seafloor sediments as shown in the Appendix 5. The X-ray diffraction test was given to all the specimens by the two methods of the unfixed direction and the fixed direction. And in order to distinguish clay minerals some of the specimens were treated with EG and HCl. The testing conditions are shown in the Table 4-3-2-1.

The minerals identified by X-ray diffraction are shown in the Table 4-3-2-2 (1) ~ (5) semi-quantitatively. In the table, ◎ indicates more than 800cps (rich), ○ indicates 800-200cps (common), △ indicates 200-100cps (poor) and + indicates less than 100cps (very poor). And when the presence of minerals is indistinct, ? is given.

The identified minerals are as follows:

Silicate minerals :

[Silica] quarts, (cristobalite?)

[Feldspar] plagioclase, albite, potash feldspar

[Zeolite] analcite, heulandite, phillipsite

[Clay minerals] chlorite, sericite, mixed layered mineral of sericite-montmorillonite, montmorillonite

Sulfate minerals : gypsum

Carbonate minerals: calcite, aragonite

Other minerals : pyrite, iron hydroxide, halite, amophous silica

The most common mineral is calcite, which is detected more than "common" in almost all the specimens. Argonite, which is also a carbonate mineral like calcite, is present in concentration in some parts (e.g. No.1-No.29, No.102-No.117) but its quantity is mostly less than "poor".

Quarts is detected in almost all the specimens. Its quantity is mostly "very poor" but in No.246-No.278 the quantity is more than "common". Feldspars are mostly plagioclace (partly albite and potash feldspar) and detected in most of the specimens, but the quanty is mostly less than "poor".

All the zeolites are detected only partially and in very small amount. Heulandite was recognized in No. 41~45 and No. 247~274. Analcite is present in No. 7~11 and No. 41~45. Phillipsite, which is commonly present in the deepsea bed sediments, is

detected in No.251-274 in concentration. Both of them (analcite and phillipsite) co-exist with heulandite.

Clay minerals are detected in almost all the specimens in trace. Of them, chlorite is most commonly detected and followed by sericite which is relatively common. It is rather rare to find mixed layered mineral of sericite-montmorillonite and montmorillonite. The specimens where both chlorite and montmorillonite are detected may include the mixed layer mineral.

Appearance of gypsum is sporadic except No. 33 ~ No. 48, and its quantity is trace.

Pyrite is very few, and is detectible in No. 6 and No. 13 only in trace. Its genetical relation with hydrothermal activities is not clear. Halite is detected in almost all the specimens, and mostly probably this is crystallized salt from the seawater through natural drying. Amorphous silica is detected in No. 37 and No. 60.

3) Statistical Analysis of Geochemical Data

The statistical analysis was performed, based on the result of geochemical data about 250 marine sediments collected in this survey area. Maximum, minimum and average values of 13 major elements are shown in Table 4-3-3-1 and them of 20 minor elements are shown in Table 4-3-3-2.

These values indicate a much variation of chemical composition as shown in Table 4-3-3-1 and Table 4-3-3-2. Most of the samples contain more than 10% of LOI. As the samples with high LOI indiate high CaO value and low LOI indicates low CaO, high LOI is considered to be derived from biogenic origin. Most of the samples indicate under detectible limitation regarding Sb and Au. At least 10 g of the sample is required to analyze Au and the accuracy of analysis is lowered in case of small amount of samples less than 10 g.

Table 4-3-3-1 Maximum, Minimum and Average Values of Major 13 Elements

Element	Max. (%)	Min. (%)	Average (%)	Element	Max. (%)	Min. (%)	Average (%)
SiO_2	70.56	10.30	37.29	CaO	42.08	1.11	17.18
TiO_2	2.70	0.01	0.53	BaO	0.47	0.01	0.04
Al_2O_3	19.14	1.22	10.24	Na_2O	6.53	2.08	3.82
Fe_2O_3	24.68	1.09	4.28	K_2O	2.78	0.32	1.10
FeO	9.20	0.26	2.14	P_2O_5	1.85	<0.01	0.21
MnO	2.53	0.02	0.34	LOI	38.72	1.53	19.64
MgO	10.35	0.81	2.38	Total	101.64	73.93	99.20

Table 4-3-3-2 Maximum, Minimum and Average Values of Minor 20 Elements

Element	Max.	Min.	Average ※1	Element	Max.	Min.	Average ※1
Ag ppm	0.54	< 0.02	0.08	Mo ppm	79.4	< 0.2	1.7
Ni ppm	163	< 1	34	Ga ppm	23	2	13
Cu ppm	116.0	4.6	45.5	Sr ppm	3675	96	718
Co ppm	37	< 1	17	Hg ppb	110	10	62
Pb ppm	22.5	0.3	3.7	Ba ppm	4220	45	345
Zn ppm	190	8	58	Au ppb	160	< 5	※2
Mn ppm	>10000	195	2480	S %	1.950	0.032	0.117
Cd ppm	1.1	< 0.1	0.2	T-R_2O_3 ppm	551	82	146
As ppm	4.0	0.4	10.1	P %	0.807	0.002	0.093
Sb ppm	3.6	< 0.2	0.3	Cl ppm	34600	800	19800

※1 Regarding a value under the detection limit, the value of each sample is half of the detection limit value. Regarding a value over the detection limit, the value of each sample is 1.5 times of the detection limit value.

※2 As almost all samples have values under the detection limit of Au, the avarage value is not calculated.

Chapter 5. The Survey of Geological Ore Deposits

5-1 Outline

Reports on active hydrothermal activities in the neighboring area, i.e. the eastern part of the Bismarck Sea, were made and related surveys were also carried out by Both et al. (1986). But surveys of this area (the western part of the Bismarck Sea) have not been made sufficiently until now. Based on such circumstances, the survey of this area was planned for this fiscal year.

The location of the spreading center was presumed, as mentioned above, from the results of the topographical survey and the magnetic survey carried out in the survey area.

In order to confirm the existence of such spreading center, the SSS survey was carried out, as mentioned later, at three track lines in the direction which crosses the assumptive spreading center obliquely. And its existence was identified. Furthermore, as the existence of submarine hydrothermal ore deposits were expected, the FDC survey was carried out at 7 track lines in the directions paralleling with the spreading center and crossing the spreading center orthogonally (as the equipment was hauled once in the middle of the operation, the actual number of track lines was eight). As the result of these surveys, ore signs or indications were discovered at five places and oxidation zones at two places. So the sampling was made at these places where ore signs or indications were discovered. Unfortunately, we could not catch any sulfide mineral by this sampling and we identified only an iron oxide zone which was presumed to be hydrothermal. Although we could not indentify any active hydrothermal activity in the survey area, we could say the fact that we discovered five ore sign zones and two oxidation zones meant that there were many traces of hydrothermal activities.

We will describe the results of SSS survey, FDC survey and sampling.

The term "ore signs or indications" was used here as an oxidation zone where we presumed, at the time of the FDC observation, that it might be accompanied by sulfides, and the simple term "oxidation zone" as an oxidation zone where we could not expect whether it was accompanied by sulfides or not.

5-2 Seafloor Topography and Geological Structure

Based on the results of the topographical survey, an intensive survey of ore doposits was carried out by centering on the following assumptive spreading centers (see Figures 3-3-1 and 5-2-1).

(1) The spreading center stretching from the Willaumez rise to the New Guinea Basin.

(2) The propagating spreading center located at the eastern part of the spreading center (1).

(3) The dying spreading center located in the south of the Willaumez rise.

(4) The spreading center located in the east of (3).

With the aim of finding out the ore signs or indications, we established the following track lines on the spreading centers (1)~(4) and carried out the FDC survey.

- Two track lines running along the central valleys and summits in the spreading center (1). (92SFDC01 & 02)
- Two track lines running along the ridges of the propagating spreading center (2). (92SFDC05 & 06)
- Two track lines roughly crossing the dying spreading center (3) orthogonally and traversing its ridges and valleys. (92SFDC07 & 08)
- Two track lines running along the valleys and ridges within the spreading center (4). (92SFDC03 & 04)

As a result of this survey, the following 5 ore signs or indications were found (see Figure 5-2-1). Oxidized sediments were mainly collected by the sampling but no sulfide minerals were obtained. Also two oxidation zones which were not clear to be accompanied by sulfide minerals were discovered at the eastern part from No. 4 ore signs.

Ore signs or indications No.1 (the spreading center (1), at the water depth of about 1,800 m). (92SFDC02)

Ore signs or indications No.2 (the spreading center (2), at the water depth of about 1,130 m). (92SFDC06)

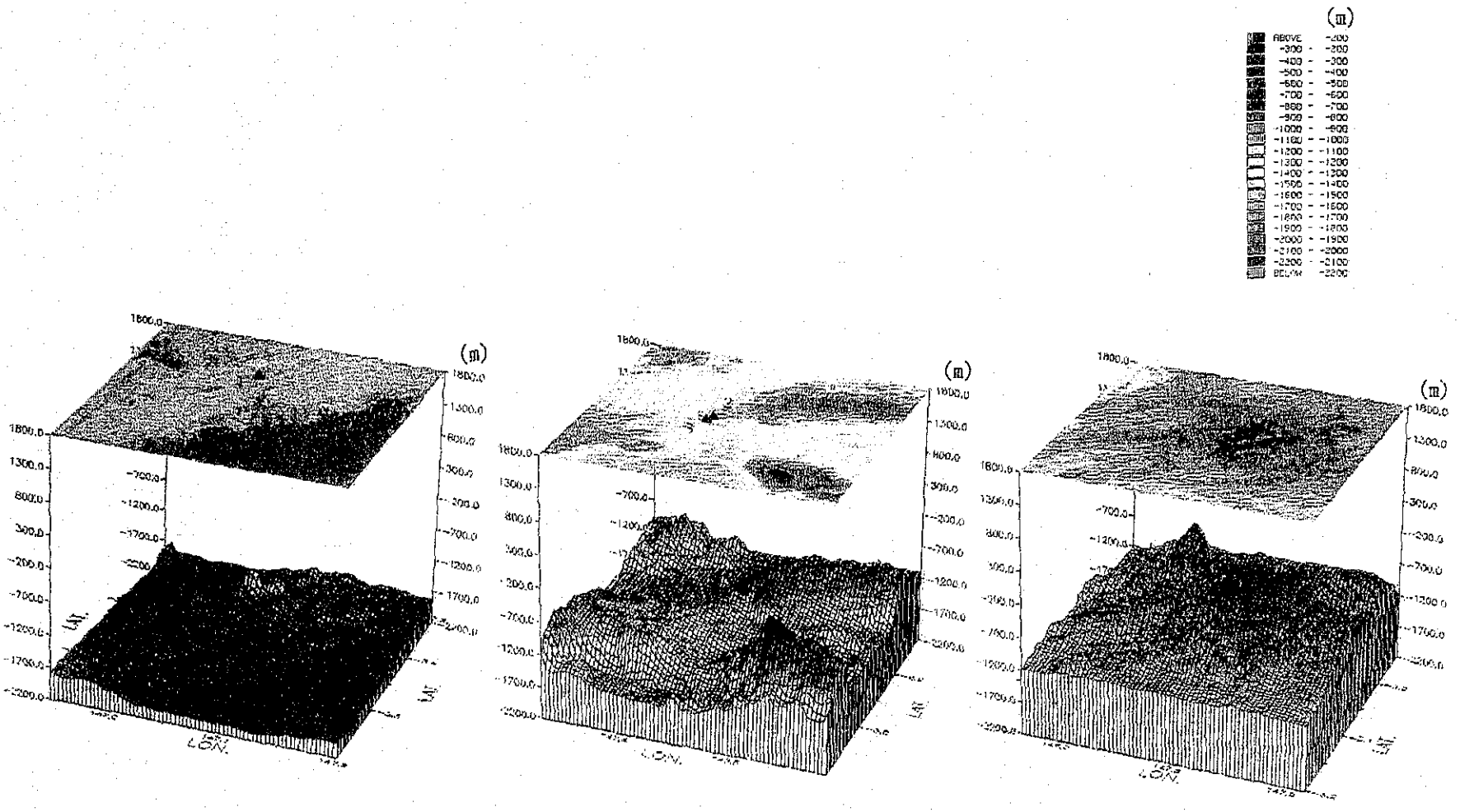

ORE SIGN No. 1

ORE SIGN No. 2 and ORE SIGN No. 3

ORE SIGN No. 4 and ORE SIGN No. 5

Figure 5-2-1 Three-dimensional Representation of a Bathymetric Map in the Neighborhood of Ore Indications. Contour labels are in meter.

Ore signs or indications No.3 (the spreading center (2), at the water depth of about 1,030 m). (92SFDC06)

Ore signs or indications No.4 (the spreading center (4), at the water depth of about 500 m). (92SFDC07)

Ore signs or indications No.5 (the spreading center (4), at the water depth of about 950 m). (92SFDC08)

Five ore signs or indications were found at the spreading centers (if we consider the propagating spreading center as identical with the spreading center), but no ore signs or indications were found at the dying spreading center. However, the FDC survey was carried out only at the two track lines, which crossed the dying spreading center orthogonally, thus the workload was scarce and the operation was not aimed at finding out ore signs or indications.

Seeing from the viewpoint of topography, the ore signs or indications No.1 was found at a central graben in the (1), the ore signs and indications Nos. 4 and 5 were found at a ridge-shaped place and a central valley in the spreading center (4), the ore signs and indications Nos. 2 and 3 were found at ridge-shaped parts of the propagating spreading center. The ore signs or indications Nos. 2, 3, 4 and 5 belong to, on the whole, seamounts and ridges. From these, ore signs or indications exist not only at the valley part but also at the ridge part. Accordingly, from the viewpoint of geological structure we can mention the seafloor spreading center as the occurrence place of mineral deposits, but we cannot identify its topographical characteristics. Furthermore, there is an example of an off axis seamount in the East Pacific Rise from which sulfide was found. So, we suggest that a survey should be done at other areas in addition to the survey of spreading centers so as to examine the occurrence place of mineral deposits.

A brief comparison between the Manus spreading center, from which sulfide ores were collected in large quantites (Tufar 1991), and the spreading centers in the survey area is described below.

The Manus spreading center (3°42'S, 149°37'E~3°00'S, 150°34'E) has water depths of 2,000 ~ 2,500 m, good linearity, and a lot of hydrothermal living things. Sulfide minerals are distributed only in the central graben of the spreading center (Tufar 1991). On the other hand, the spreading center (1) has water depths of 700 ~ 1,750 m and a small difference in relative height among ridges. The width of the ridges is irregular and the central graben is intermittent (see Figures 5-2-2 and 5-2-3). The spreading center (4) has very shallow water depths of about 500 m.

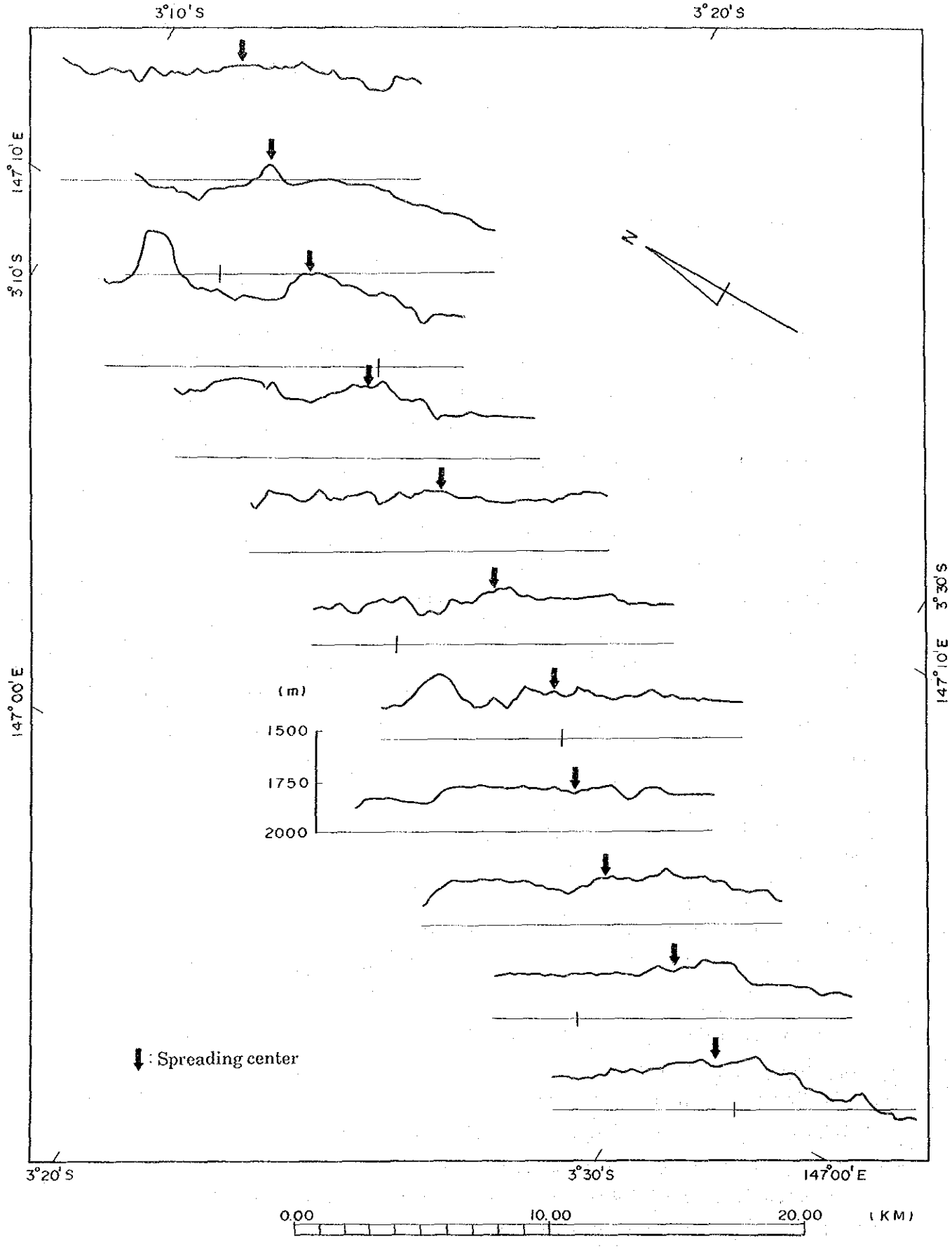

Figure 5-2-2 Bathymetric Profiles in the Region of the Spreading Center

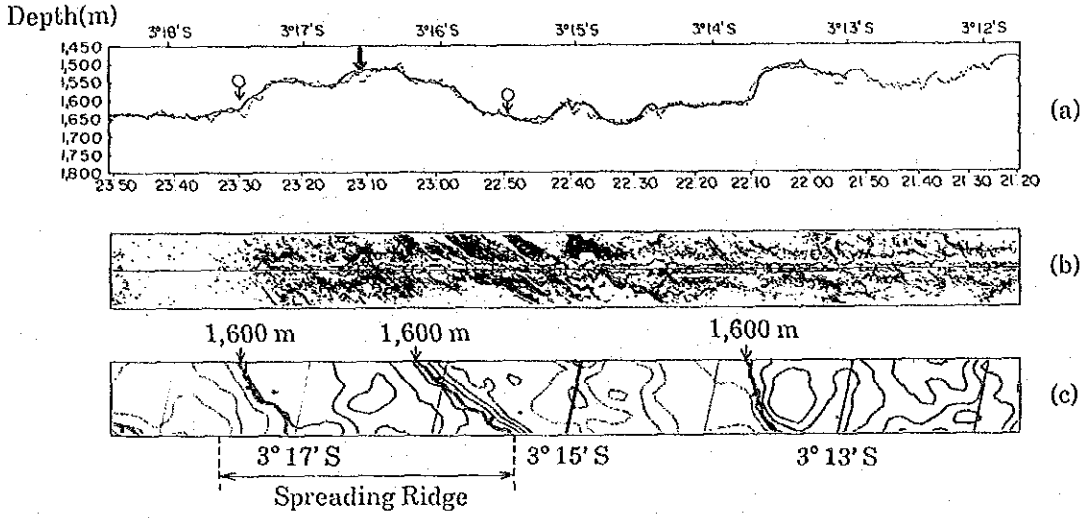

(1) 92SSSS01

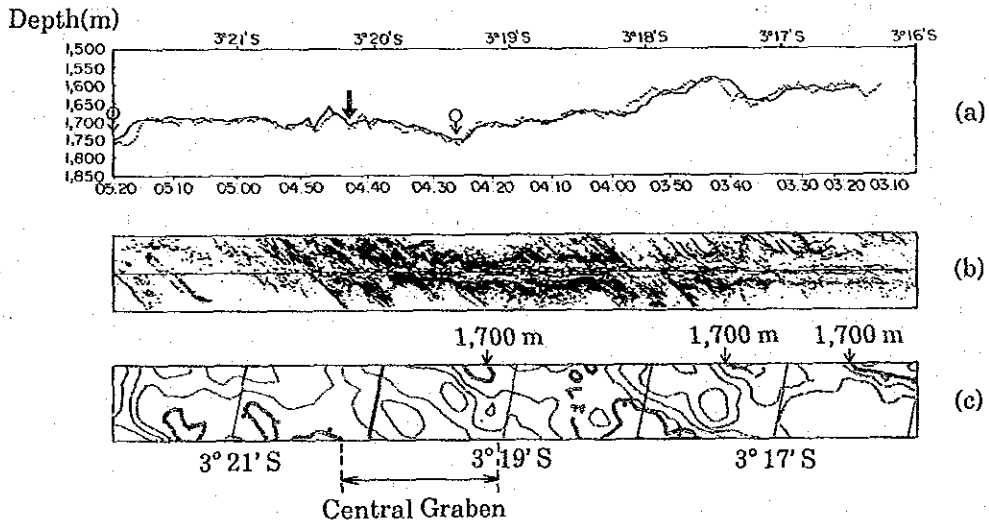

(2) 92SSSS02

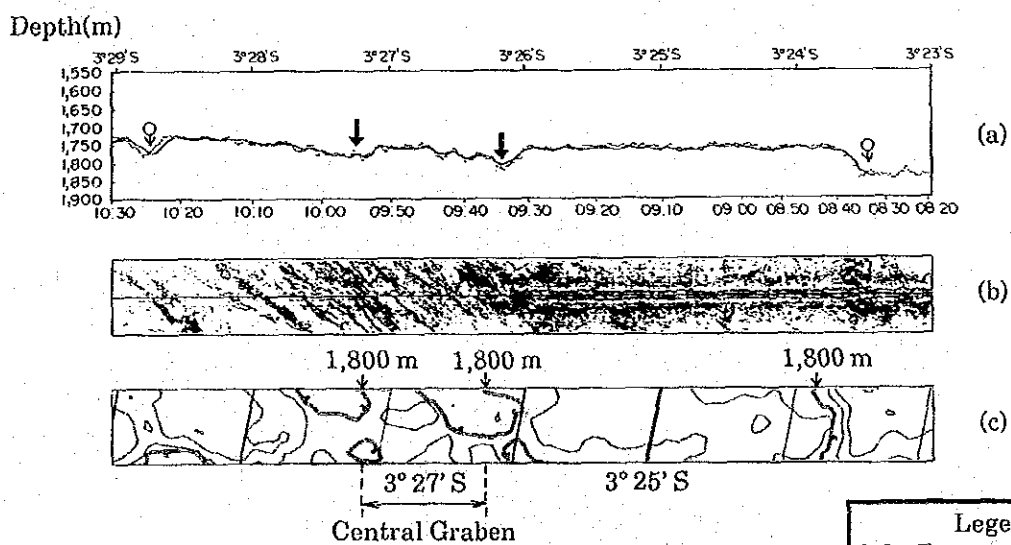

(3) 92SSSS03

(a) : The depth profile by SSS and NBS
(b) : Sidescan Image
(c) : Bathymetric map based on MBES

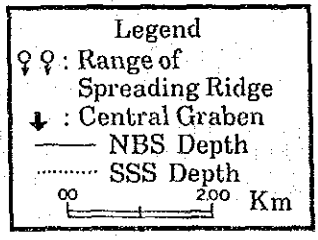

Figure 5-2-3 Results of Sidescan Sonar Survey

Furthermore, the water temperature anomaly on the spreading centers (1)~(4) is not clear and no hydrothermal living things are recognized. So, it is not clear whether these spreading centers (1)~(4) are in activity now.

The results of the sidescan sonar (SSS) survey aiming at determing the middle of the spreading center (1) is shown in Figure 5-2-3. Topographically saying, the relative height difference of the ridges is small, so this one is a place hard to determine whether it is a spreading center.

When performing the SSS survey, the track line was established in the way that the track line would cross the spreading center obliquely with the aim to identify the spreading center (ridge) clearly, so the width of the ridge was slightly wider than the actual width. Basically, we determined the furrow registered with a strong oblique reflection pattern as the central graben (Figure 5-2-3).

The ridge (spreading center) is distinct but its central graben is not clear (92S·SSS01). The relative height of the spreading center (ridge) is small but there is a central graben composed of a stepped fault (oblique reflection pattern) (92S·SSS02). The width of the ridge is considerably wide which infers the existence of two central grabens (92S·SSS03). Finally, these results correspond well to the results of MBES.

5-3 Seafloor Geology

1) Survey Results by FDC

As the FDC sea floor observation, color photographs and color VTR were taken simultaneously with at the presumptive sea floor spreading center. Location of all track lines are shown in Figure 5-3-1-1, route-maps of each track line are shown in Annexed Figure 4 (1) ~ (6) and location of each track line are shown in Annexed Figure 5 (1) ~ (6). And typical sea floor photographs are shown in Figure 5-3-1-2. The results of the FDC survey are shown in Table 5-3-1-1 (1), (2). The results of each track line are as follows:

<Track line 92SFDC01>

Details of the observation time, location and number of photographs taken are as follows:

Starting point	: 3°15.75'S, 147°09.85'E
Terminal point	: 3°22.04'S, 147°05.14'E
Bearing	: 216.6°
Distance	: 7.9 miles
Depth	: 1,506~1,839 m
Starting time	: 00:43 on Sept. 7, 1992 (GMT)
Ending time	: 07:47 on Sept. 7, 1992 (GMT)
Duration	: 7 hours and 4 minutes
Number of photographs	: 210

This track line was established along with the axial of the ridges presumed from the results of morphological analysis. The location of the track line is shown in Annexed Figure 4 (1), route-map is shown in Annexed Figure 5 (1).

Sandy ~ muddy sediments are relatively prominent on this track line. The ratio between the duration, of which outcropped rock was recognized, and of which sediments was done was roughly 1:1. Sandy ~ muddy sediments assume dark colors. These sediments are distributed over rocks but rocks are often outcropped from under the sediments. From which, the thickness of these sediments is considered to be relatively thin. No ripple marks are recognized. Rocks are mainly composed of pillow lava, but sheet lava and talus sediments are partially recognized. Pillow lava assume pillow shape ~ tube-shape (rich in expansion and contraction). Average diameter of each pillow is 1~2m. It has ropy structure on the surface together with

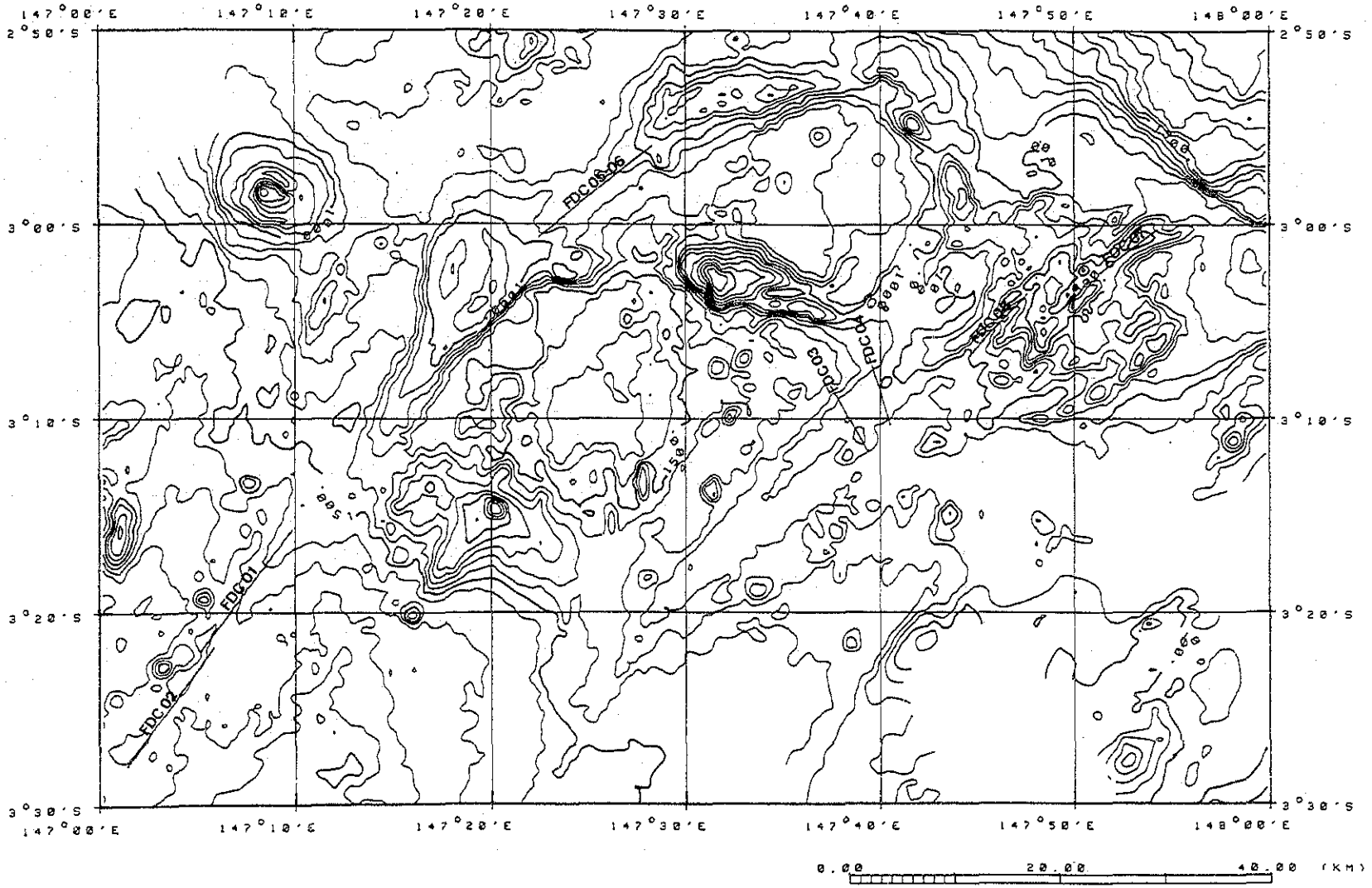

Figure 5-3-1-1 Location Map of FDC Lines (General View)

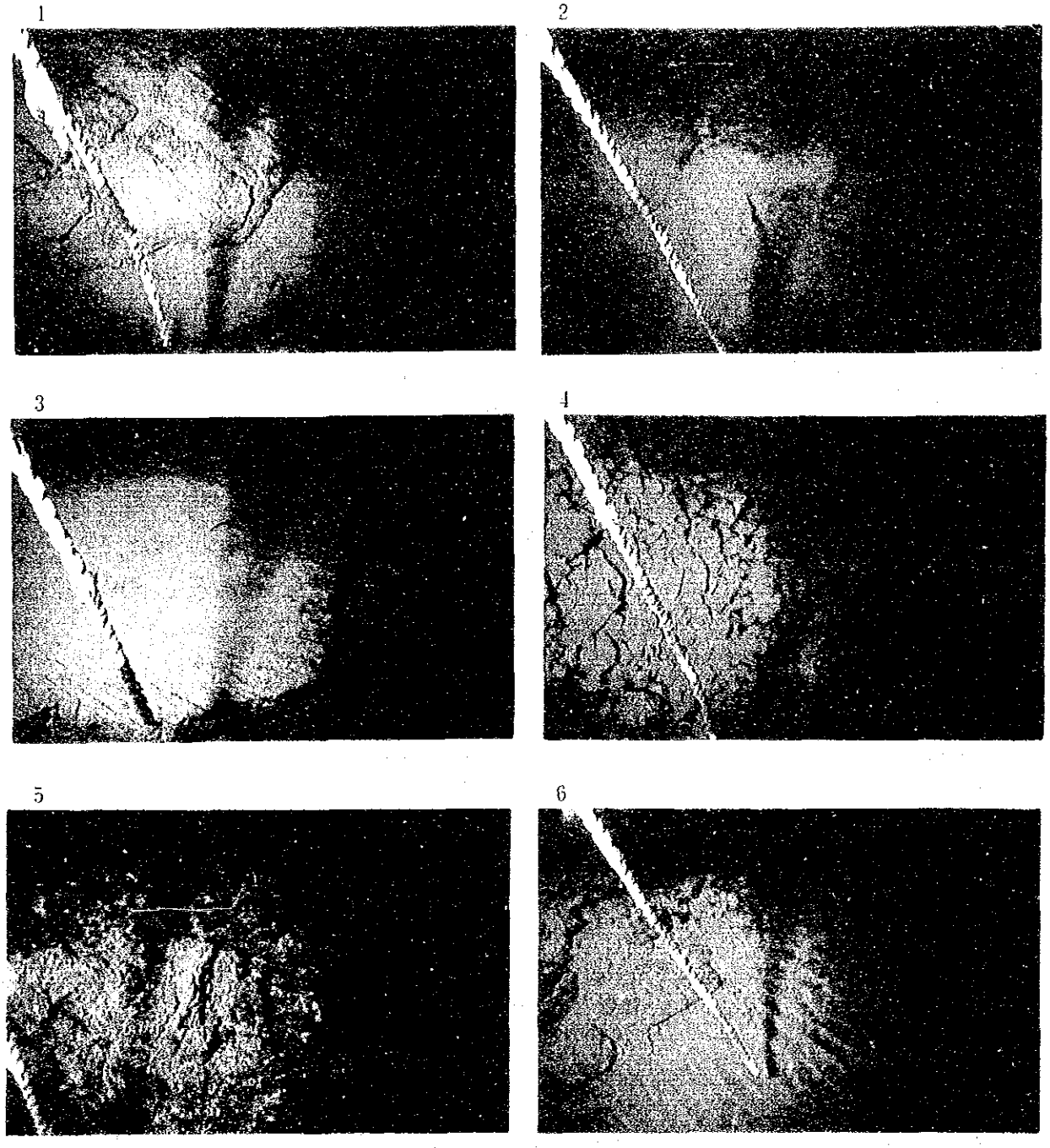

1. Pillow lava (pillow shape) Line 92SFDC04 (3°09.67'S, 147°40.33'E, water depth 1,061m)
2. Pillow lava (tube shape) Line 92SFDC04 (3°07.97'S, 147°39.81'E, water depth 1,027m)
3. Sheet lava Line 92SFDC06 (3°00.36'S, 147°22.82'E, water depth 1,088m)
4. Talus sediments Line 92SFDC06 (2°57.16'S, 147°26.75'E, water depth 1,085m)
5. Slaggy lava Line 92SFDC07 (3°01.69'S, 147°52.32'E, water depth 517m)
6. Ripple marks Line 92SFDC08 (3°03.79'S, 147°47.30'E, water depth 606m)

Figure 5-3-1-2 Seafloor Photographs taken by FDC

Table 5-3-1-1 List of the Results of FDC (1)

Date	Track Line No.	※	Time	Location		Depth (m)	Survey Duration (hrs) (a~d)	Observation duration (hrs) (b~c)	Observation length (mile)	Number of photos	Description
				Latitude	Longitude						
9/ 7	92SFDC01	a	00:32				7:19	7:04	7.9	210	Observed along the spreading center. Sandy/muddy sediments:rock exposure =1:1. Sandy/muddy sediments are relatively thin. Rocks consist of mainly pillow lava, and partially of sheet lava and talus sediments. Pillow lava is barrel-shaped or tube-shaped with full of expansions and contractions, and has ropy structure and contraction cracks. Phenomena which indicate hydrothermal ore deposits are not detected. Common living things on hydrothermal activities are not detected.
		b	00:43	3' 15.75' S	147' 09.85' E	1,506					
		c	07:47	3' 22.04' S	147' 05.14' E	1,839					
		d	07:51								
9/ 7	92SFDC02	a	22:37				6:37	6:23	7.2	171	Observed along the spreading center. Sandy/muddy sediments:rock exposure =1:1. Sandy/muddy sediments are relatively thin. Rocks consist of mainly pillow lava, and partially of sheet lava and talus sediments. Pillow lava is barrel-shaped or tube-shaped with full of expansions and contractions, and has ropy structure and contraction cracks. Yellow sediments thought to be iron hydro-oxide was discovered at one place (150m). Common living things on hydrothermal activities are not detected.
		b	22:47	3' 21.80' S	147' 05.84' E	1,760					
9/ 8		c	05:10	3' 27.62' S	147' 01.63' E	1,829					
		d	05:14								
9/ 8	92SFDC03	a	22:34				3:10	2:48	3.2	81	Observed rectangularly across the spreading center. Sandy/muddy sediments:rock exposure=1:2. Sandy/muddy sediments are relatively thin. Rocks consist of mainly pillow lava, and partially of sheet lava and talus sediments. Pillow lava is barrel-shaped or tube-shaped with full of expansions and contractions, and has ropy structure and contraction cracks. Phenomena which indicate hydrothermal ore deposits are not detected. Common living things on hydrothermal activities are not detected.
		b	22:49	3' 08.80' S	147' 37.75' E	1,015					
		c	01:37	3' 11.56' S	147' 39.29' E	1,114					
9/ 9		d	01:44								
9/ 9	92SFDC04	a	03:08				3:03	2:42	3.0	81	Observed rectangularly across the spreading center. Sandy/muddy sediments:rock exposure=1:2. Sandy/muddy sediments are relatively thin. Rocks consist of mainly pillow lava, and partially of sheet lava and talus sediments. Pillow lava is barrel-shaped or tube-shaped with full of expansions and contractions, and has ropy structure and contraction cracks. Phenomena which indicate hydrothermal ore deposits are not detected. Common living things on hydrothermal activities are not detected.
		b	03:19	3' 07.19' S	147' 39.56' E	975					
		c	06:01	3' 10.07' S	147' 40.44' E	1,096					
		d	06:11								

※: a:Throwing Time, b:arriavl Time on Seafloor, c:Taking Time off Seafloor, d:Haul-in Time
Note: Date and time are in GMT. Location and depth of the towing vehicle were calculated from the vessel position by GPS, the winch length and water depth by NBS or CTD.

Table 5-3-1-1 List of the Results of FDC (2)

Date	Track Line No.	※ a b c d	Time	Location		Depth (m)	Survey Duration (hrs) (a~d)	Observation duration (hrs) (b~c)	Observation length (mile)	Number of photos	Description
				Latitude	Longitude						
9/ 9	92SFDC05	a	22:20				1:13	0:52	0.9	37	Observed along the spreading center. Observation was suspended due to malfunction of the stroboscope. Connected to the 06 track line.
		b	22:34	2°55.79' S	147°28.43' E	890					
		c	23:26	2°56.39' S	147°27.71' E	1,012					
		d	23:33								
9/10	92SFDC06	a	01:01				6:06	5:40	6.5	194	Observed along the spreading center. Sandy/muddy sediments:rock exposure =1:3. Sandy/muddy sediments are relatively thin. Rocks consist of mainly pillow lava, and partially slaggy lava. Pillow lava is barrel-shaped or tube-shaped with full of expansions and contractions, and has ropy structure and contraction cracks. Yellow sediments thought to be iron hydroxide was discovered at two places (30m and 100m continuation respectively). Common living things on hydrothermal activities are not detected.
		b	01:12	2°56.30' S	147°27.81' E	1,004					
		c	06:52	3°00.38' S	147°22.80' E	1,160					
		d	07:07								
9/10	92SFDC07	a	22:09				3:22	3:03	3.4	161	Observed along the spreading center. Sandy/muddy sediments hardly exist. Rocks consist mainly of talus and fine-pebble sediments, which are porous and composed of slaggy detritus of several meters-several centimeters long, having a parallel vein structure. Brown sediments thought to be iron hydro-oxide were recognized at two places (500m and 700m continuation respectively), and brown sediments thought to be ore sings were recognized at one place (350m continuation).
		b	22:19	3°00.32' S	147°54.16' E	341					
9/11		c	01:22	3°02.34' S	147°51.47' E	532					
		d	01:31								
9/11	92SFDC08	a	02:25				3:55	3:31	3.7	138	Observed along the spreading center. Sandy/muddy sediments:rock exposure =1:3. Rocks consist mainly of sheet lava and partially of pillow lava and slaggy lava. Slaggy lava is porous and lumpy with the size of several meters, having parallel vein structure. Brown sediments thought to be iron hydro-oxide were discovered at one place (550m continuation). Common living things on hydrothermal activities are not detected.
		b	02:39	3°03.66' S	147°47.44' E	578					
		c	06:10	3°06.32' S	147°44.90' E	968					
		d	06:20								

※: a:Throwing Time, b:arrival Time on Seafllor, c:Taking Time off seafloor, d:Haul-in Time
Note: Date and time are in GMT. Location and depth of the towing vehicle were caluculated from the vessel position by GPS, the winch length and water depth by NBS or CTD.

radial cracks resulted from contraction. Sheet lava has vesicular and parallel striped structure. It often occurs as a mass of rock in the scale of several meters and transition to slag lava or aa lava is often made.

Any phenomenon indicating the existence of hydrothermal ore deposits on this track line was not recognized macroscopically.

Living things observed on this track line include such Echinodermata as crinoids, starfishes, sea urchins and sea cucumbers, such Coelenterata as actiniaria, and fishes and shrimps. A lot of holes with diameters of several centimeters - presumed to be trace fossils - were recognized on sandy ~ muddy sediments. Also, pieces of wood transported from the land were frequently observed.

<Track line 92SFDC02>

Details of the observation time, location and number of photographs taken are as follows:

Starting point	: 3°21.80'S, 147°05.84'E
Terminal point	: 3°27.62'S, 147°01.63'E
Bearing	: 216.0°
Distance	: 7.2 miles
Depth	: 1,760~1,829m
Starting time	: 22:47 on Sept. 7, 1992 (GMT)
Ending time	: 05:10 on Sept. 8, 1992 (GMT)
Duration	: 6 hours and 23 minutes
Number of photographs	: 171

This track line was established on a southwestward extension from the track line 92SFDC01 along with the axial of the ridges presumed from the results of morphological analysis. The location of the track line is shown in Annexed Figure 4 (2), route-map is shown in Annexed Figure 5 (2).

As in the case of the track line 92SFDC01, sandy ~ muddy sediments are relatively prominent on this track line. The ratio between the duration, of which outcropped rock was recognized, and of which sediments was done was roughly 1:1. Sandy ~ muddy sediments assume dark colors. These sediments are distributed over rocks but rocks are often outcropped from under the sediments. From which, the thickness of these sediments are considered to be relatively thin. No ripple marks are recognized. Rocks are mainly composed of pillow lava but sheet lava and talus sediments are partially recognized. Pillow lava assumes pillow shape ~ tube-shape

(rich in expansion and contraction). Average diameter of each pillow is 1~2 m. It has ropy structure on the surface together with radial cracks resulted from contraction. Sheet lava has vesicular and parallel striped structure. It often occurs as a mass of rock in the scale of several meters and transition to slag lava or aa lava is often made. Talus sediments are often composed of slightly roundish rock with a diameter of scores centimeters.

Yellowish sediments considered to be iron oxide or lava altered by oxidation are intermittently observed for about 5 minutes (for a distance of about 150m) in the neighborhood of 3°24.7'S, 147°03.8'E on this track line (No.1 ore sign or indication).

Living things observed on this track line include such Echinodermata as crinoids, starfishes, sea urchins and sea cucumbers, such Coelenterata as actiniaria, and fishes and shrimps. A lot of holes with diameters of several centimeters - presumed to be trace fossils - were recognized on sandy ~ muddy sediments. Also, pieces of wood transported from the land were frequently observed.

<Track line 92SFDC03>

Details of the observation time, location and number of photographs taken are as follows:

Starting point	: 3°08.80'S, 147°37.75'E
Terminal point	: 3°11.56'S, 147°39.29'E
Bearing	: 150.4°
Distance	: 3.2 miles
Depth	: 1,015~1,114 m
Starting time	: 22:49 on Sept. 8, 1992 (GMT)
Ending time	: 01:37 on Sept. 9, 1992 (GMT)
Duration	: 2 hours and 48 minutes
Number of photographs	: 81

This track line was established in the direction of orthogonalizing the axial of the ridges presumed from the results of morphological analysis. The location of the track line is shown in Annexed Figure 4 (3), route-map is are shown in Annexed Figure 5 (3).

Outcropped rocks are prominent at this track line and the range recognized with sandy ~ muddy sediments is small. The ratio of observation time between the former (rocks)and the latter (sediments) is roughly 2:1. Sandy ~ muddy sediments assume dark colors. These sediments are distributed over rocks but rocks are often

outcropped from under the sediments. From which, the thickness of these sediments are considered to be relatively thin. No ripple marks are recognized. Rocks are mainly composed of pillow lava, and sheet lava and talus sediments are recognized at extremely rare intervals. Pillow lava assume pillow shape ~ tube-shape (rich in expansion and contraction). Average diameter of each pillow is 1~2 m. It has ropy structure on the surface together with radial cracks resulted from contraction.

Any phenomenon indicating the existence of hydrothermal ore deposits on this track line was not recognized macroscopically.

Living things observed on this track line include such Echinodermata as crinoids, starfishes, sea urchins and sea cucumbers, such Coelenterata as actiniaria, and fishes and shrimps. A lot of holes with diameters of several centimeters - presumed to be trace fossils - and faculas or white spots with diameters of about 10 cm were recognized on sandy ~ muddy sediments. Also, pieces of wood transported from the land were observed at rare intervals.

<Track line 92SFDC04>

Details of the observation time, location and number of photographs taken are as follows:

Starting point	: 3°07.19'S, 147°39.56'E
Terminal point	: 3°10.07'S, 147°40.44'E
Bearing	: 162.6°
Distance	: 3.0 miles
Depth	: 975~1,096 m
Starting time	: 03:19 on Sept. 9, 1992 (GMT)
Ending time	: 06:01 on Sept. 9, 1992 (GMT)
Duration	: 2 hours and 42 minutes
Number of photographs	: 81

This track line was established on the northwestern side of the track line 92SFDC03 in the direction of orthogonalizing the axial of the ridges presumed from the results of morphological analysis. The location of the track line is shown in Annexed Figure 4 (3), route-map is shown in Annexed Figure 5 (3).

Contrary to the track line 92SFDC03,sandy ~ muddy sediments are relatively prominent and the range recognized with outcropped rocks is small. The ratio of observation time between the former and the latter is roughly 2:1. Sandy ~ muddy

sediments assume dark colors. These sediments are distributed over rocks but rocks are often outcropped from under the sediments. From which, these sediments are considered to be relatively thin. No ripple marks are recognized. Rocks are mainly composed of pillow lava, and sheet lava and talus sediments are recognized at extremely rare intervals. Pillow lava assume pillow shape ~ tube-shape (rich in expansion and contraction). Average diameter of each pillow is 1~2m. It has ropy structure on the surface together with radial cracks resulted from contraction.

Any phenomenon indicating the existence of hydrothermal ore deposits was not recognized macroscopically on this track line.

Living things observed on this track line include such Echinodermata as crinoids, starfishes, sea urchins and sea cucumbers, such Coelenterata as actiniaria, and fishes and shrimps. A lot of holes with diameters of several centimeters - presumed to be trace fossils - and faculas or white spots with diameters of about 10 cm were recognized on sandy ~ muddy sediments. Also, pieces of wood transported from the land were observed at rare intervals.

<Track line 92SFDC05>

Details of the observation time, location and number of photographs taken are as follows:

Starting point	: 2°55.79'S, 147°28.43'E
Terminal point	: 2°56.39'S, 147°27.71'E
Bearing	: 230.2°
Distance	: 0.9 miles
Depth	: 890~1,012 m
Starting time	: 22:34 on Sept. 9, 1992(GMT)
Ending time	: 23:26 on Sept. 9, 1992(GMT)
Duration	: 52 minutes
Number of photographs	: 37

This track line was established in the direction along with the axial of the ridges presumed from the results of morphological analysis but due to the malfunction of the stroboscope, the observation was suspended and the equipment was hauled in the middle course. As the remaining program was observed at the track line 92SFDC06, the results were described in the paragraph of 92SFDC06.

<Track line 92SFDC06>

Details of the observation time, location and number of photographs taken are as follows:

Starting point	: 2°56.30'S, 147°27.81'E
Terminal point	: 3°00.38'S, 147°22.80'E
Bearing	: 230.6°
Distance	: 6.5 miles
Depth	: 1,004~1,160 m
Starting time	: 01:12 on Sept. 10, 1992(GMT)
Ending time	: 06:52 on Sept. 10, 1992(GMT)
Duration	: 5 hours and 40 minutes
Number of photographs	: 194

This track line is the succession to the track line 92SFDC05, the observation of which was suspended and the equipment was hauled in in the middle course due to the malfunction of the stroboscope. The location of the track line is shown in Annexed Figure 4 (4), route-map is shown in Annexed Figure 5 (4).

Outcropped rocks are relatively prominent on this track line and the range recognized with sandy~muddy sediments is small. The ratio of observation time between the former and the latter is roughly 3:1. Sandy ~ muddy sediments assume dark colors. These sediments are distributed over rocks but rocks are often outcropped from under the sediments. From which, these sediments are considered to be relatively thin. No ripple marks are recognized. Rocks are mainly composed of pillow lava, and slag lava is recognized partially, but sheet lava and talus sediments are recognized at extremely rare intervals. Pillow lava assume pillow shape ~ tube-shape (rich in expansion and contraction). Average diameter of each pillow is 1~2m. It has ropy structure on the surface together with radial cracks resulted from contraction. Slag lava has a vesicular and coarse surface, and irregular morphology.

Ore signs or indications were spotted at the following two sites on this track line. Yellowish sediments presumed to be iron oxide were recognized between pillow lava for about one minute of the observation time (for a distance of about 30m) in the vicinity of 2°56.7'S, 147°27.3'E (No.2 ore sign or indication). Also, yellowish sediments presumed to be iron oxide or oxidized and altered slag lava were recognized intermittently for about 3 minutes of the observation time (for a distance of about 100m) in the vicinity of 2°57.3'S, 147°26.6'E (No.3 ore sign or indication).

Living things observed on this track line include such Echinodermata as crinoids, starfishes, sea urchins and sea cucumbers, such Coelenterata as actiniaria, and fishes and shrimps. A lot of holes with diameters of several centimeters - presumed to be trace fossils - and faculas or white spots with diameters of about 10 cm were recognized on sandy ~ muddy sediments. Also, pieces of wood transported from the land were universally observed.

<Track line 92SFDC07>

Details of the observation time, location and number of photographs taken are as follows:

Starting point	: 3°00.32'S, 147°54.16'E
Terminal point	: 3°02.34'S, 147°51.47'E
Bearing	: 233.1°
Distance	: 3.4 miles
Depth	: 341~532m
Starting time	: 22:19 on Sept. 10, 1992(GMT)
Ending time	: 01:22 on Sept. 11, 1992(GMT)
Duration	: 3 hours and 3 minutes
Number of photographs	: 161

This track line was established in the direction along with the axial of the ridges presumed from the results of morphological analysis. The location of the track line is shown in Annexed Figure 4 (5), route-map is shown in Annexed Figure 5 (5).

Outcropped rocks are prominent on this track line and the range recognized with sandy ~ muddy sediments is extremely small. Rocks are mainly composed of talus ~ brecciatd deposits. Although pillow lava and slag lava are recognized partially but they are distriburd locally. Talus ~ brecciated deposits are composed of slag lava with lengths of several meters to several centimeters and have vesicular and parallel striped structure. Their sorting is extremely bad.

Two oxidation zones were recognized as follows on this track line. Brown precipitates presumed to be iron oxide and green clay were recognized intermittently among talus sediments for about 15 minutes of the observation time (for a distance of about 500 m) in the vicinity of 3°00.5'S, 147°53.9'E. Brown precipitates presumed to be iron oxide or plate-shaped oxidized and altered brown precipitates were recognized intermittently for about 20 minutes of the observation time (for a distance of about 700 m) in the vicinity of 3°01.8'S, 147°52.2'E. Also, yellow precipitates persumed to be ore signs or indications, or

plate-shaped oxidized and altered brown precipitates were recognized intermittently for about 10 minutes of the observation time (for a distance of about 50 m) in the vicinity of 3°02.2'S, 147°51.6'E on this track line (No. 4 ore sign or indication).

Living things observed on this track line include such Echinodermata as crinoids, starfishes, sea urchins and sea cucumbers, such Coelenterate as actiniaria, and fishes and shrimps. A lot of small red crabs with a length of less than 5 cm were recognized among vesicular talus ~ brecciated deposits. Also, pieces of wood transported from the land were universally observed.

<Track line 92SFDC08>

Details of the observation time, location and number of photographs taken are as follows:

Starting point	: 3°03.66'S, 147°47.44'E
Terminal point	: 3°06.32'S, 147°44.90'E
Bearing	: 223.5
Distance	: 3.7 miles
Depth	: 578~968 m
Starting time	: 02:39 on Sept. 11, 1992(GMT)
Ending time	: 06:10 on Sept. 11, 1992(GMT)
Duration	: 3 hours and 31 minutes
Number of photographs	: 138

This track line was established in the direction along with the axial of the depressed zone parallel to the ridges presumed from the results of morphological analysis. The location of the track line is shown in Annexed Figure 4 (6), route-maps are shown in Annexed Figure 5 (6).

Outcropped rocks are prominent on this track line and the range recognized with sandy ~ muddy sediments is small. The ratio of observation time between the former and the latter is roughly 3:1. Rocks are mainly composed of sheet lava, pillow lava and slag lava are partially recognized. Sheet lava occurs frequently as a mass of rock of several meters scale with vesicular and parallel striped structure, and transition to slag lava or aa lava is not uncommon. The surface structure of slag lave is vesicular and coarse and the morphology of slag lava is irregular. Pillow lava assume pillow shape ~ tube-shape (rich in expansion and contraction). Average diameters of each pillow are 1~2 m. Pillow lava has ropy structure on the surface together with radial cracks resulted from contraction. Sheet lava ~ slag

lava tend to range in shallower part and pillow lava in deeper part. Sandy ~ muddy sediments assume light grey colors and ripple marks are universally recognized on their surface. Vesicular talus ~ brecciated deposits are universally transited to each other.

Brown precipitates presumed to be iron oxide and plate-shaped oxidized and altered precipitates are intermittently recognized for about 17 minutes of the observation time (for a distance of about 550 m) in the vicinity of 3°06.0'S, 147°45.1'E on this track line (No.5 ore sign or indication).

Living things observed on this track line include such Echinodermata as crinoids, starfishes, sea urchins and sea cucumbers, such Coelente rata as actiniaria, and fishes and shrimps. A lot of small red crabs with a length of less than 5 cm were recognized among vesicular talus ~ brecciated deposits. Also, pieces of wood transported from the land were observed at rare intervals.

2) Properties of the Collected Rocks

The sampling for the ore deposit survey was carried out at six points among the sea-floor surfaces from which ore signs or indications and an oxidation zone had been recognized by the FDC survey. Okean grab and power grab were employed for the sampling. These sampling locations are shown in Annexed Figure 6. Among the samples collected by this sampling operation, rocks ran up to 2,200 kg (see Appendix Table 3). Photographs of representative rocks are shown in Figure 5-3-2-1.

Collected rocks are composed of basalt and scoriae.

Most of the basalt has black vitric film on its surface. This vitric film is considered to be the effects of the contact with seawater. The surface of the film part is generally smooth and shows conchoidal fractures and glassy luster, but occasionally, it has cracks resulting from contraction. The average thickness of this film part is 2~10 mm, but, on rare occasions, it reaches 50 mm. The inner part of the basalt is fine-grained, without megaphenocryst and assumes black - dark grey. And, usually, it is vesicular with many long and narrow voids - the length of which is less than 2 cm - forming the concentric shape. Iron oxides assuming reddish brown and sticking on the surface of the basalt are recognized.

Furthermore, oolitic chlorite sticking on the inner part of the basalt is recognized. From this fact, the existence of cavitated lava can be expected. The basalt collected by the FDC frame during the survey at the track line 92SFDC04 is black

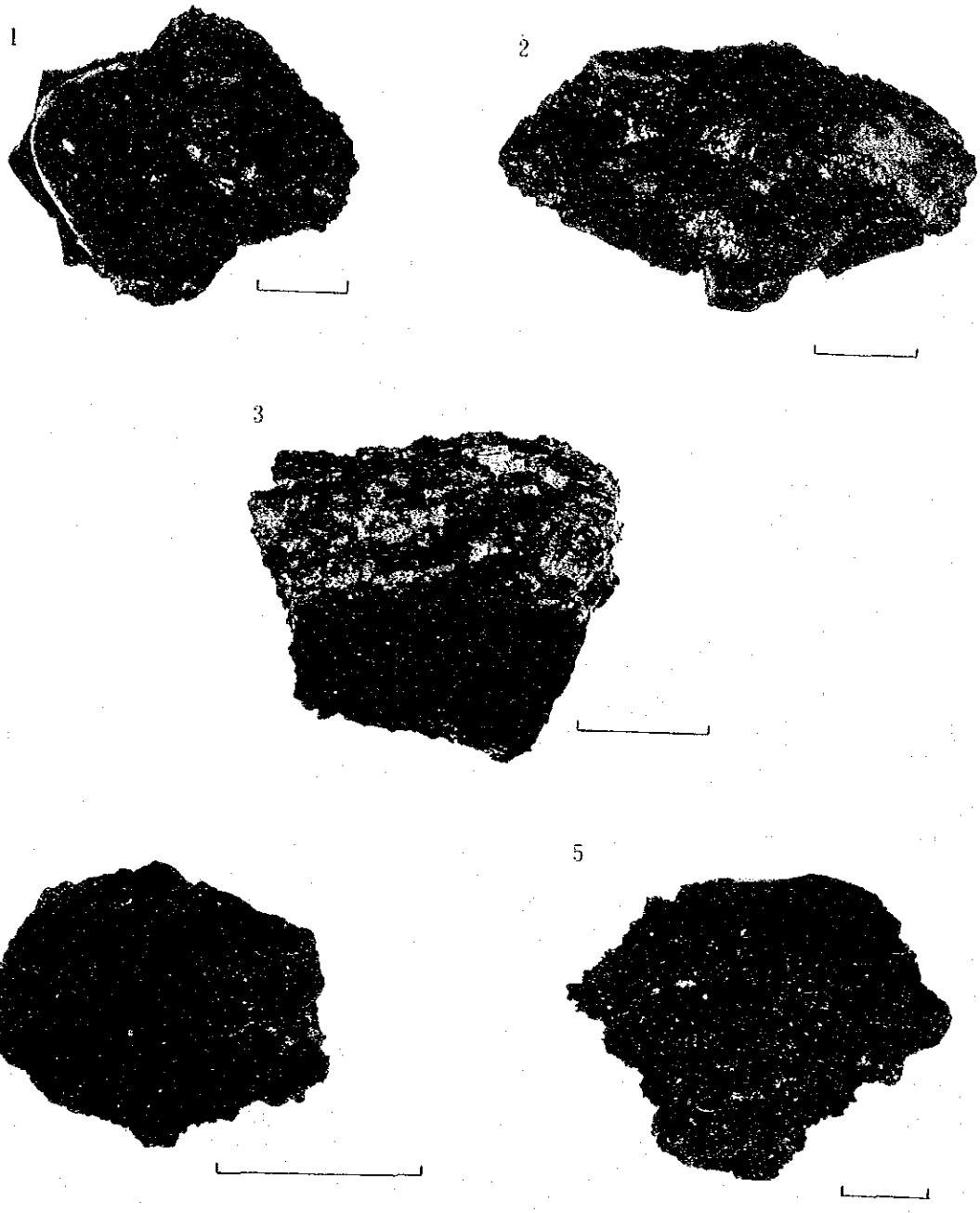

Note: Each scale bar is 5cm.

1. Hyline film on surface layer of basalt (92HPG18)
2. Hyline surface and inside adhered by ferrous oxides (92HPG08)
3. Oolitic chlorites are attached in the inside of basalt (92HPG19)
4. Scoria (92HPG08)
5. Slaggy lava (92HPG12)

Figure 5-3-2-1 Photos of Substrates (Investigation of Mineral Deposits)